Intron-mediated enhancement boosts Rtn4 circRNA expression: A robust method for exploring circRNA function

Dingding Mo[#, *], Xinping Li[#]
#, Max Planck Institute for Biology of Ageing, Joseph-Stelzmann-Strasse 9b, 50931 Cologne, Germany
*, Corresponding author, Dingding Mo, Dingding.Mo@age.mpg.de

Abstract:
CircRNAs are expressed in many important biological processes. Studying their function requires an effective expression method. When we used intron-mediated enhancement (IME) to improve circRNA expression of the mouse Rtn4 (Nogo, a key protein in Nogo-Rho pathways) circRNA as a test case, we achieved a 4-6-fold improvement compared to an existing method. We further developed this approach into a general circRNA expression vector pCircRNA-DMo. An unexpected feature of our approach is its ability to promote translation of circRNA into detectable amounts of proteins. Intriguingly, both monomer and multimer peptides can be observed as a result of rolling circle translation of RTN4 circRNA. We also confirmed the presence of both peptide forms in human and mouse brains, highlighting the significance of circRNA translation *in vivo*. In summary, we demonstrate the significant advantage of IME in enhancing circRNA biogenesis and hence our vector offers a robust platform for exploring potential circRNA peptide-encoding functions.

Key words: Rtn4 CircRNA, Nogo, Nogo-Rho pathways, circRNA translation, Intron-mediated enhancement (IME), chimeric intron, IVS1, PAT1, pCircRNA-DMo, rolling cycle of translation, monomer and repeating peptides.

Introduction:

Circular RNAs (circRNA) are 5' and 3' covalently jointed isoforms from pre-mRNA back-splicing (Hentze and Preiss 2013; Vicens and Westhof 2014; Chen 2016). They may play important roles in various biological processes, especially in brain development and ageing (Westholm et al. 2014; Rybak-Wolf et al. 2015; Veno et al. 2015; You et al. 2015; Gruner et al. 2016). For example, Cdr1as/ciRS-7 (circular RNA sponge for miR-7) can bind miR-7 and regulate its activity (Hansen et al. 2013; Memczak et al. 2013; Piwecka et al. 2017). The function of circRNAs in cancer is also increasingly recognized (Guarnerio et al. 2016; Kristensen et al. 2017; Xia et al. 2017).

Over-expression of circRNA is achieved by constructing inverted repeats in the 5' and 3' flanking intron sequences of the circularized exon (Hansen et al. 2013; Liang and Wilusz 2014; Zhang et al. 2014). Since circularization competes with classic splicing, over-expression of circRNA is typically less efficient than for linear forms (Ashwal-Fluss et al. 2014; Starke et al. 2015; Zhang et al. 2016). Moreover, the accumulation of large amounts of linear precursor without efficient splicing may disturb circRNA-specific expression (Legnini and Bozzoni 2017).

Intron-mediated enhancement (IME) is a conserved phenomenon across eukaryotes, including plants and mammals, where the expression of a gene is enhanced by an intron, often located upstream, and close to the start of transcription (Brinster et al. 1988; Buchman and Berg 1988; Huang and Gorman 1990; Choi et al. 1991; Palmiter et al. 1991; Rose and Beliakoff 2000; Gallegos and Rose 2015). Although the precise mechanism of IME is still largely unknown, the enhancement of mRNA accumulation from an intron-containing gene is often highly significant, and is frequently used as a powerful method to increase gene expression, especially in transgenic organisms (Gallegos and Rose 2015; Laxa 2016). However, it is unknown whether IME can also enhance circRNA expression.

Reticulon-4, also known as neurite outgrowth inhibitor (Nogo-A, B, C), encoded by the RTN4 gene, is an inhibitor of neurite outgrowth in the central nervous system of higher vertebrates, and may play critical role in blocking neuroregeneration after brain injury (Schwab 2010; Seiler et al. 2016). RTN4 circRNA comprising exon 2 and 3 of the RTN4 gene is expressed in both human and mouse brain at detectable levels (Rybak-Wolf et al. 2015), thus representing a good model for studying circRNA expression.

We generated an IME circRNA expression vector and used it to increase the expression levels of Rtn4 circRNA in cell lines. Furthermore, we confirmed that such a vector is a general method for enhancing circRNA biogenesis by testing two additional IME introns. Finally, we show that boosted circRNA can be translated into proteins, demonstrating the significance of this method for studying circRNA function.

Material and methods:

Plasmid construction

To construct the Rtn4 circRNA expression plasmid, Rtn4 circRNA exon genomic region (chr11: 29, 704, 497-29, 708, 881, mouse GRCm38/mm10) along with the 5' and 3' flanking intronic sequences were amplified from N2a cell genomic DNA and inserted under the CMV promoter in pCMV-MIR (OriGene) vector. 800 nucleotides of 5' intronic regions (chr11:29,704,521-29,705,320) were reverse complementary inverted and added to the 3' of the intron to promote the back-splicing (Hansen et al. 2013; Rybak-Wolf et al. 2015). As the flanking introns lacks the 5' and 3' splice sites respectively, they would not be able to perform classic splicing to generate liner mRNA. The resulting construct was called pCircRNA-BE-Rtn4. To generate completely identical circRNA without additional sequences from restriction endonuclease sites in the circRNA expression vector, we performed overlap PCR instead of using restriction endonucleases in the plasmid construction. pCircRNA-DMo-Rtn4 was constructed based on pCircRNA-BE-Rtn4 with the addition of a chimeric intron from the pCI-neo-FLAG vector (kindly provided by Niels Gehring, University of Cologne) to the upstream of circRNA expression region under the same CMV promoter.

To create general circRNA expression vectors, multiple restriction endonuclease sites (BglII, NheI, BmtI, EcoRV, NotI, SacII, XbaI) were added to the original Rtn4 circRNA exon of pCircRNA-BE-Rtn4 or pCircRNA-DMo-Rtn4, producing the vectors for other circRNA expression, called pCircRNA-BE or pCircRNA-DMo (Supplementary Fig. 1).

The chimeric intron of pCircRNA-DMo-Rtn4 was replaced with the IVS1 intron or PAT1 intron 1 to generate pCircRNA-IVS1-Rtn4 and pCircRNA-PAT1-Rtn4 constructs (Buchman and Berg 1988; Rose and Beliakoff 2000). The linear mRNA expression of Rtn4 exon 2-exon3 was achieved by insertion of mouse Rtn4 exon 2-intron 2-exon 3 into pCMV-MIR vector under the CMV promoter and the resulting construct was called pCMV-Rtn4-Exon 2-Exon 3. A FLAG tag (DYKDDDDKPP) and stop codon (TGA) were added to the middle of exon 2 of pCircRNA-DMo-Rtn4 plasmid to form pCircRNA-DMo-Rtn4-FLAG and pCircRNA-DMo-Rtn4-Stop.
Details of the oligos used in plasmid constructions are provided (Supplementary table). All constructs were verified by DNA sequencing. Plasmid DNAs used in mammalian cell transfection were purified with an EndoFree Plasmid Maxi Kit (QIAGEN).

Cell culture and plasmid DNA transfection

Mouse neuro 2a cell line (N2a) was purchased from Sigma. The N2a-swe.10 cell line (N2a cells stably expressing c-Myc epitope-tagged APP_{Swe}) was kindly provided by Gopal Thinakaran from The University of Chicago. HeLa and HEK293 cells were kindly provided by Nils-Göran Larsson at the Max Planck Institute for Biology of Ageing. N2a, HeLa, HEK293 were cultured in Dulbecco's modified Eagle medium (DMEM, Invitrogen), supplemented with 10% foetal bovine serum (Gibco), 10 mM sodium pyruvate (Sigma), 100 U/ml penicillin and 100 U/ml streptomycin (Gibco) at 37 °C in 5% (v/v) CO_2. N2a-swe.10 cells were cultured in special medium described previously(Thinakaran et al. 1996).
For transfection, 2.5 µg of plasmid DNA diluted in 150 µl Opti-MEM (Invitrogen) was mixed with 5 µl lipofectamine 2000 diluted in 150 µl Opti-MEM and the resulting transfection mix was added to about 0.5 million cells in 6 well plates. After 24 hours, the transfection mix was transferred to fresh DMEM medium. After 3 to 6 days of transfection, cells were collected for total RNA isolation and total protein extraction.

Total RNA isolation and qRT-PCR

Total RNAs from N2a, N2a-swe.10, HeLa and HEK 293 cells were isolated using TRIzol reagent (Ambion) according to the manufacturer's recommendations. 0.5 μg of total RNA was used to synthesize cDNA by random oligos with the SuperScript®III First-Strand Synthesis System (Invitrogen). Quantitative PCR amplification was performed using a 7900HT Fast Real Time PCR System (Applied Biosystems) using the Power SYBR Green PCR Master Mix (Applied Biosystems). Fold expression differences between treated samples versus control samples were calculated using the $2^{-\Delta\Delta C}{}_{T}$ method with β-Actin mRNA as internal control (Livak and Schmittgen 2001).

Western blot assays

Total protein from HEK293, N2a cells and mouse frontal cortex samples was prepared in RIPA buffer (50mM Tris-HCl pH 8.0, 150 mM NaCl, 0.1% (w/v) SDS, 0.5% (w/v) Na-Deoxycholate, 1% (v/v) NP40, 1* Roche cOmplete Protease Inhibitor and 1* PhosSTOP Phosphatase Inhibitor). Human brain samples were purchased from BioCat GmbH. 40 µg of total protein was fractioned on SDS-PAGE with reducing loading buffer (5% β-mercaptoethanol) and transferred to nitrocellulose membranes (Amersham), then immunoblotted against Nogo-A (Rtn4, 1:1000, #13401, Cell signalling Technology) and β-Actin (1: 15000; A5441, Sigma).

Blots were then incubated with horseradish peroxidase conjugated secondary antibodies (goat-anti-rabbit, IgG (H+L), G21234; goat-anti-mouse IgG (H+L), G21040; Life technologies) and developed with ECL solution (Amersham) and imaged with the ChemiDoc MP Imaging System (Bio-Rad).

Label-free quantitative proteomics

HEK293 cells individually transfected with pCircRNA-BE-Rtn4, pCircRNA-DMo-Rtn4 and the control empty plasmid were lysed and digested in solution with trypsin according to a previously established method (Li and Franz 2014). Briefly, cell pellets were heated and sonicated in lysis buffer (100 mM Tris-HCl, 6 M guanidinium chloride (guanidine hydrochloride, GuHCl), 10 mM TCEP (Tris (2-carboxyethyl) phosphine), 40 mM CAA (chloroacetamide)). After centrifugation, the diluted supernatant proteins were digested by trypsin (Promega, V5280) overnight and the resulting peptides were purified with C18-SD StageTip (Kulak et al. 2014; Li and Franz 2014). The prepared peptides were analysed by an Orbitrap Fusion mass spectrometer (Thermo Fisher Scientific) with a nano-electrospray ion source, coupled with an EASY-nLC 1000 (Thermo Fisher Scientific) UHPLC. MaxQuant version 1.5.3.8 with an integrated Andromeda search engine was used to analyse the LC-MS/MS raw data (Cox et al. 2011; Kulak et al. 2014). Detailed method is provided (Supplementary method).

Results

Expression of Rtn4 circRNA using an existing method

A mouse Rtn4 circRNA expression cassette was amplified from N2a genomic DNA and constructed as previously described by Hansen et al. (Hansen et al. 2013). It included 800-nucleotide reverse complementary repeats in the 5' and 3' flanking intronic regions, and was inserted into the pCMV-MIR vector under the CMV promoter (Fig. 1A). Transfection of the resulting Rtn4 circRNA expression construct, pCircRNA-BE-Rtn4 (basal expression), into mouse neuroblastoma cell line (N2a) and its derivative, N2a-swe.10, followed by qRT-PCR with Rtn4 circRNA-specific PCR oligos (Rtn4-c-F and Rtn4-c-R, Fig. 1A) showed that Rtn4 circRNA over-expression was 3.9/5.8-fold higher than endogenous expression, i.e. after empty vector transfection (Fig. 1B). In two kinds of human cell lines, HeLa and HEK293, pCircRNA-BE-Rtn4 also expressed Rtn4 circRNA. Overall the flanking intronic sequences with inverted repeats can moderately promote Rtn4 circRNA biogenesis, thus serving as a good starting cassette for further optimizing circRNA vector design.

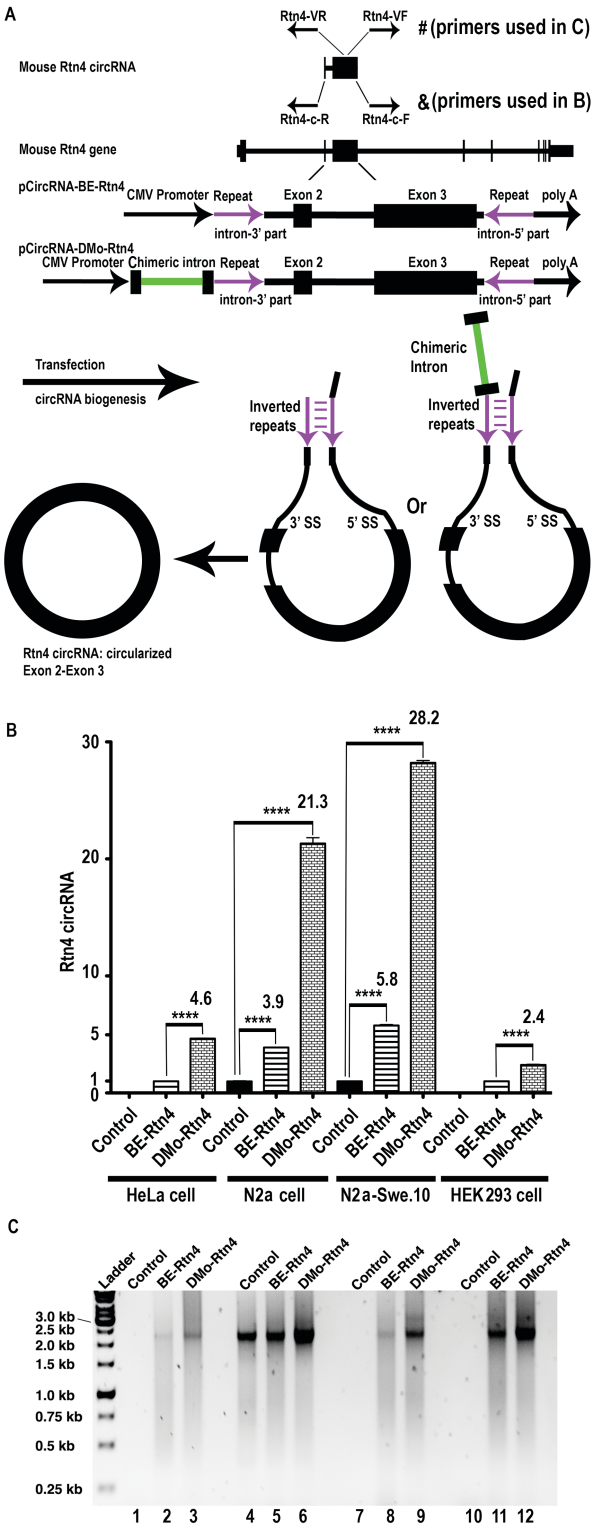

Fig. 1. Mouse Rtn4 circRNA structure and expression in mammalian cells

A. Scheme of Rtn4 circRNA sequence localization in the Rtn4 gene and CircRNA expression cassette from pCircRNA-BE and pCircRNA-DMo vectors; mouse Rtn4 circRNA consists exon 2 and exon 3 of Rtn4 gene. 800 nts inverted repeats (purple colour) in the flanking introns were constructed to promote back-splicing through forming inter-intronic base-pairing; the flanking introns lacks 5' and 3' splice site respectively which would abolish the classic splicing of exon 2 and exon 3; chimeric intron was shown in green; & and #, the Rtn4 circRNA RT-PCR oligo

positions; &, Rtn4-c-R, Rtn4-c-F were used in qRT-PCR to determine Rtn4 circRNA levels (results shown in B); #, Rtn4-VR, Rtn4-VF were used to verify Rtn4 circRNA back-splicing fidelity (results shown in C).
B. Rtn4 circRNA expression levels in transfected cells (HeLa, N2a, N2a-swe.10, HEK293 cell); Control = pCMV-MIR empty vector; BE-Rtn4 = pCircRNA-BE-Rtn4; DMo-Rtn4 = pCircRNA-DMo-Rtn4; All statistic T tests were performed by comparison with the control sample, ****, $P \leq 0.0001$, $n \geq 4$; β-Actin mRNA was used as internal control.
C. Agarose gel electrophoresis of RT-PCR products of Rtn4 circRNA to verify back-splicing fidelity (PCR primers: Rtn4-VR, Rtn4-VF); Control = pCMV-MIR empty vector; BE-Rtn4 = pCircRNA-BE-Rtn4; DMo-Rtn4 = pCircRNA-DMo-Rtn4. The spliced circular form of Exon 2 and exon 3 without intron is 2418 nt. The size of Intron between two exons is 818 nt. The expected amplicon size is 2401 bp. As the products migrated between 2.0 and 2.5 kb, proving that the internal intron was spliced out in Rtn4 circRNA biogenesis. lane 1-3, HeLa cells; lane 4-6, N2a cells; lane 7-9, N2a-swe.10 cells; lane 10-12, HEK293 cells. PCR products were sequenced (data not shown);

A neighbouring chimeric intron significantly enhances Rtn4 circRNA biogenesis: Intron-mediated enhancement (IME) in circRNA expression

The presence of an intron frequently increases mRNA accumulation in gene expression, described as intron-mediated enhancement (IME) (Gallegos and Rose 2015; Laxa 2016). An interesting question is whether the neighbouring intron can also promote circRNA expression. To test this, we amplified a chimeric intron that has shown a strong IME effect in mRNA expression from pCI-neo vector (Promega) and inserted it upstream of the Rtn4 circRNA cassette under the same CMV promoter (Fig. 1A). The resulting vector was called pCircRNA-DMo-Rtn4.

Expression studies in N2a and N2a-swe.10 showed that Rtn4 circRNA biogenesis was significantly improved from 4-6-fold up to 21-28-fold, representing robust enhancement of circRNA expression (Fig. 1B). The IME effect on Rtn4 circRNA expression in the two kinds of human cell lines, HeLa and HEK293 resulted a 4.6/2.4-fold increase in Rtn4 circRNA expression in these cells with the chimeric intron vector (pCircRNA-DMo-Rtn4), compared to the intron-less control (pCircRNA-BE-Rtn4), thus demonstrating that the chimeric intron-containing circRNA expression vector drives ubiquitous enhancement effects in various cell lines (Fig. 1B). Our data clearly show that intron-mediated enhancement (IME) boosts circRNA expression, thus providing a good strategy for circRNA expression cassette construction.

Back-splicing fidelity of pCircRNA-BE-Rtn4 and pCircRNA-DMo-Rtn4
Next, we evaluated the back-splicing fidelity of our circRNA expression vectors. As shown above, the unique RT-PCR oligos (Rtn4-VF, Rtn4-VR in Fig. 1A) could amply the full sequence of Rtn4 circRNA. Agarose gel electrophoresis of the RT-PCR product showed that expressed Rtn4 circRNAs were all the same size (Fig. 1C). Further sequencing of the RT-PCR products confirmed that the Rtn4 circRNA sequences were identical to the wild type circRNAs without any sequence differences in either human or mouse cell lines (data not shown).

We conclude that both of our expression vectors produce circRNA with the same sequence as the endogenous copy, representing high back-splicing fidelity.

IVS1 and PAT1 introns also boost circRNA biogenesis: Ubiquitously robust enhancement by various introns

To further test whether the IME effect on circRNA expression is universal to different introns, we replaced the chimeric intron in pCircRNA-DMo-Rtn4 with two other introns, IVS1 and PAT1 intron 1, which were shown to stably enhance their cognate mRNA expression (Buchman and Berg 1988; Rose and Beliakoff 2000). The resulting Rtn4 circRNA expression vectors, pCircRNA-IVS1-Rtn4 and pCircRNA-PAT1-Rtn4 (Fig. 2A) were transfected into N2a cells, and the qRT-PCR of Rtn4 circRNA showed that IVS1 and PAT1 introns enhance Rtn4 circRNA expression from 3.9-fold (pCircRNA-BE-Rtn4) to 7.8 and 6.8-fold, representing about 2-fold enhancement, although not as robustly as the ca. 20-fold enhancement driven by pCircRNA-DMo-Rtn4 (Fig. 2A, B).

Based on these results, we conclude that various introns could boost circRNA, demonstrating the universal existence of the IME effect in circRNA biogenesis.

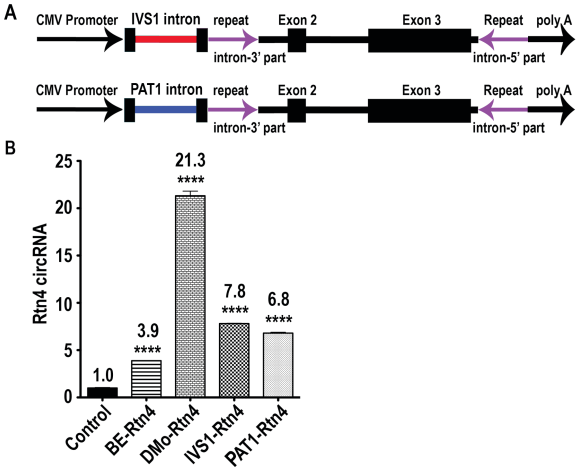

Fig. 2. Expression of Rtn4 circRNA with IVS1 and PAT1 introns

A. Scheme of the Rtn4 circRNA expression cassette for pCircRNA-IVS1-Rtn4 and pCircRNA-PAT1-Rtn4 constructs. IVS1 intron was shown in red colour and PAT1 intron was shown in blue colour.

B. Rtn4 circRNA expression in N2a cells after transfection with Rtn4 circRNA constructs.

All statistic T tests were performed by comparison with the control sample, ****, $P \leq 0.0001$, ***, $P \leq 0.001$, $n \geq 4$.

Protein product from Rtn4 circRNA

To investigate the coding potential of circRNAs, we performed Western blots using Anti-Nogo A antibody to detect proteins in the Rtn4 circRNA overexpressing cells. Since there was very weak / no expression of endogenous RTN4 protein in HEK 293 cells, we chose these cell extracts as controls for the Rtn4 circRNA translation study. As a positive control, we used pCMV-Rtn4 exon 2-3 (Fig. 3A), which expresses a linear counterpart mRNA of the Rtn4

circRNA exons. The translated protein from Rtn4 exon 2-3 mRNA migrated at around 150 kDa in the Western blot (Fig. 3C). The pCircRNA-BE-Rtn4 product failed to produce detectable protein, but pCircRNA-DMo-Rtn4 not only clearly expressed an Rtn4 related protein of around 150 kDa in HEK293 cells, but interestingly also a much larger form, possibly due to repeating peptides expressed from continuous translation, as discussed below (Fig. 3B). These results mirror the dramatic induction of expression of Rtn4 circRNA due to the IME effect.

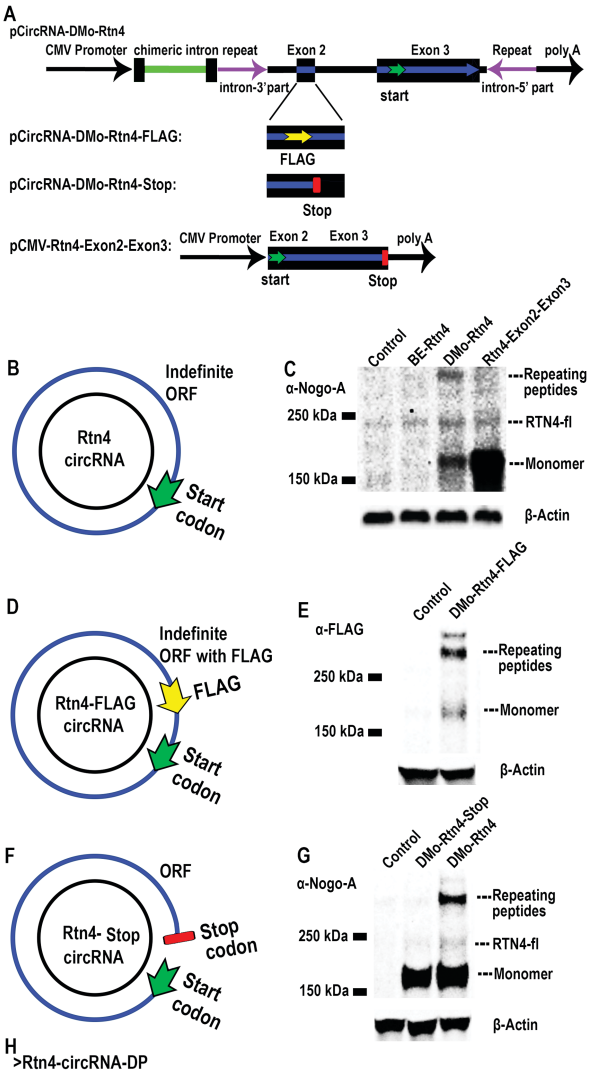

Fig. 3. Rolling circle translation of Rtn4 circRNA

A. Scheme illustrating the insertion of a FLAG tag and stop codon into exon2 of the open reading frame of Rtn4 circRNA. Blue, open reading frame; green arrow, start codon; yellow arrow, FLAG tag in the pCircRNAsDMo-Rtn4-FLAG construct; red rectangle, stop codon in the pCircRNA-DMo-Rtn4-Stop construct.

B. Indefinite open reading frame (ORF) of Rtn4 circRNA.

C. Western blot of Rtn4 circRNA translated proteins in HEK293 cell detected by antibodies against Nogo-A (α-Nogo-A). Control, empty vector; BE-Rtn4 = pCircRNA-BE-Rtn4; DMo-Rtn4 = pCircRNA-DMo-Rtn4; Rtn4-Exon2-Exon3 = pCMV- Rtn4-Exon2-Exon3. On the right repeating peptides are multimers of the Rtn4 circRNA translation product; RTN4-fl indicates the endogenous RTN4 full length protein (Nogo-A); monomer is the single round translation product of Rtn4 circRNA.
D. Open reading frame of Rtn4-FLAG circRNA.
E. Western blot of pCircRNA-DMo-Rtn4-FLAG transfected N2a cells using an anti-FLAG antibody (α-FLAG). Control, the empty vector; DMo-Rtn4-FLAG = pCircRNA-DMo-Rtn4-FLAG.
F. Open reading frame of Rtn4-stop circRNA.
G. Western blot of pCircRNA-DMo-Rtn4-Stop transfected HEK293 cells using an anti-Nogo A antibody (α-Nogo-A). Control, the empty vector; DMo-Rtn4-Stop = pCircRNA-DMo-Rtn4-Stop; DMo-Rtn4 = pCircRNA-DMo-Rtn4.
H. Mass spectrometry results of Rtn4 circRNA derived peptides (Rtn4-circRNA-DP) expressed in HEK293 cell. The predicted sequence of monomer mouse Rtn4 circRNA derived peptides; red sequences, the detected peptides (detailed peptide spectrometry was provided in Supplementary Fig. 2).

The indefinite translation of Rtn4 circRNA

Examination of the open reading frame of Rtn4 circRNA found that this circRNA does not have a stop codon, so represents a circular ORF that may produce repeating peptides, with potentially very high molecular weight. As predicted, we observed a high molecular weight band in the Western blot against Rtn4 protein in pCircRNA-DMo-Rtn4 transfected HEK293 cells under reducing condition (Fig. 3C). These large proteins presumably arise from Rtn4 circRNA continuous translation (Fig. 3B). To further verify the specificity of these large proteins, and that they resulted from circRNA translation, we added a FLAG tag to the 5' part of Rtn4 circRNA to generate pCircRNA-DMo-Rtn4-FLAG (Fig. 3D). Since the FLAG tag was located upstream of the start codon in the construct, FLAG can only be expressed from circular translation of Rtn4 circRNA (Fig. 3A, D). Western blotting for the FLAG tag detected both the monomer and high molecular weight bands of large proteins, further suggesting the continuous translation of the circular ORF of Rtn4 circRNA (Fig. 3A, D, E). As these large proteins with high molecular weight may also rise from protein aggregation of the monomer (although with less possibility), we then added a stop codon into the middle of exon 2 (pCircRNA-DMo-Rtn4-Stop, Fig. 3A, F), Western blot analysis with anti-Nogo-A antibody revealed that the stop codon abolished these high molecular bands (DMo-Rtn4-Stop in Fig. 3G), while the monomer of Rtn4 circRNA translated protein remained. If these high molecular weight bands were from protein aggregation, the stope code addition should not affect their migration. Thus, the abolishing of high molecular bands by stop codon addition in the ORF solidly confirmed the expression of repeating peptides from the continuous translation of Rtn4 circRNA.

To further investigate the identity of the peptides derived from Rtn4 circRNA translation, we performed shotgun mass spectrometry of Rtn4 peptides overexpressed in HEK293 cells. We detected 17 unique peptides (Supplementary Fig. 2), which covered about 38% of the putative translated monomer protein sequence from Rtn4 circRNA (the red sequences in Fig. 3H,). Since

the putative protein sequence from mouse Rtn4 circRNA translation is significantly different from the counterpart human RTN4 protein fragment (Supplementary Fig. 3), we could confirm that peptides detected by mass spectrometry were derived from mouse Rtn4 circRNA translation. Moreover, since the peptide coverage is good, we are fairly confident that the genetic code used in Rtn4 circRNA translation is as same as that used for linear mRNA (Fig. 3H, Supplementary Fig. 2).

In summary, we conclude that Rtn4 circRNA is translated into monomer and mutimer peptides. Similarly, we observed that the chimeric intron could induce Rtn4 circRNA production and hence elevated translation products in N2a cells (Supplementary Fig. 4). Furthermore, IVS1 and PAT1 introns could also elevate both the expression level of Rtn4 circRNA and its translated protein in N2a cells (Supplementary Fig. 4). Taken together, we conclude that IME could significantly enhance gene expression of circRNAs.

***In vivo* translation of endogenous RTN4 circRNA in human and mouse brain**

Since RTN4 circRNA has been detected in human and mouse brain, we then asked whether it is translated *in vivo*. Western blot analysis of human and mouse brain tissues using an anti-Nogo-A antibody detected both the monomer and repeating peptides from RTN4 circRNA translation along with the full length RTN4 protein (Fig. 4), demonstrating the indefinite translation of RTN4 circRNA *in vivo*.

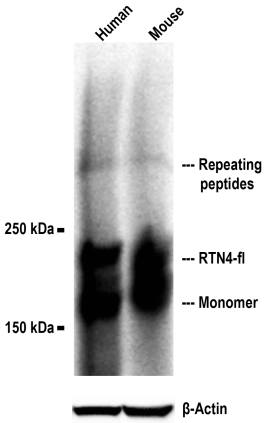

Fig. 4. RTN4 circRNA-derived peptides expressed in human and mouse brain.

Human brain frontal lobe and mouse frontal cortex samples were fractioned by SDS-PAGE and immunoblotted against Nogo-A (α-Nogo-A). RTN4-fl, RTN4 full length protein (Nogo-A); monomer, monomer of RTN4 circRNA derived peptide; repeating peptides, multimer of RTN4 circRNA derived peptide. β-Actin was used as a loading control.

Discussion

Perhaps the most intriguing question about circRNAs concerns their functions. Although several hypotheses have been proposed, the biological roles of most circRNAs are still elusive. Previous studies on circRNA functions have been hampered by the lack of an efficient molecular tool to alter their expression levels. Using three different neighbouring introns, we

clearly demonstrate that intron-mediated enhancement (IME) can boost circRNA expression. Interestingly, since the majority of highly expressed circRNAs are derived from the middle exons of host genes (Zhang et al. 2014), their flanking introns may have IME effects that promote corresponding circRNA expression. Here, we propose that IME represents a dramatically improved method to accelerate studies into circRNA function.

CircRNAs are mostly hosted by protein encoding genes and produced by back-splicing in parallel to the linear counterpart mRNA splicing. Since these RNA species are located mostly in the cytoplasm, an attractive and immerging idea is that circRNAs may serve as templates for protein synthesis.

Previous studies have shown that several *in vitro* synthesized circular RNAs can be translated *in vitro* and in cells (Chen and Sarnow 1995; Abe et al. 2015). An artificial split GFP circRNA can produce intact GFP protein (Wang and Wang 2015). Furthermore, it has been shown that endogenous circ-ZNF609 circRNA can be translated into protein in a cell line (Legnini et al. 2017). A circRNA generated from the muscleblind locus is reported to encode a protein in a drosophila fly's head (Pamudurti et al. 2017). N6-methyladenosine (m6A) modification of circRNA could induce efficient initiation of protein translation of circRNAs (Yang et al. 2017). These findings highlight the possibility that many, if not most circRNAs are translatable, hence acting similarly as their linear counterpart mRNA (Tatomer and Wilusz 2017).

Here, we show that IME can significantly elevate Rtn4 circRNA production, thus offering a better expression tool for investigating the functions of circRNA, especially protein synthesis. We have recently used pCircRNA-DMo vector to express two other circRNAs in cell lines. Preliminary result show that IME can significantly improve their expressions (Dingding Mo, unpublished data).

Interestingly, we demonstrate that Rtn4 circRNA is translated into monomer and multimer peptide forms, representing rolling circle translation of an indefinite ORF. Importantly, the expression of both monomer and repeating peptides from RTN4 circRNA translation in human and mouse brain highlight their significance *in vivo*. Such unique rolling cycle translation had previously been described in an artificial circRNA (Chen and Sarnow 1995; Abe et al. 2015). Here, we confirm its existence in natural circRNA. Such a finding indicates that other circRNAs may also have indefinite ORFs, thus adding new dimensions to RNA translation. Interestingly, peptides species from the indefinite ORF of RTN4 circRNA are limited (Fig. 3), indicating that there is an unknown mechanism to terminate the translation from the circular RNA even without the stop codon. It will be fascinating to ask how repeating peptides are synthesised by ribosomes and how they are folded.

So far, we do not know whether such RTN4 circRNA-derived proteins are functionally important. Since RTN4 protein is an important neurite outgrowth inhibitor and a key protein in Nogo-Rho pathways, antagonizing RTN4 full-length protein is one of the approaches being investigated in neuroregenerative medicine (Schwab and Strittmatter 2014). Since the second exon of the RTN4 circRNA encodes the Δ 20 domain mediating neurite growth inhibition (Schwab 2010), RTN4 circRNA-derived proteins containing the Δ 20 domain may also inhibit neurite growth and represent new players in Nogo-Rho pathways.

In summary, we conclude that IME provides robust benefits for circRNA gene expression, thus serving as an excellent tool to investigate various circRNA functions. However, further study is required to decipher the mechanism of how IME boosts circRNA expression and subsequent translation. Specifically, in terms of RTN4 circRNA, it may prove to be a clinically relevant tool to investigate the function of RTN4 circRNA-derived proteins.

Acknowledgements

The authors acknowledge the department of biological mechanisms of ageing led by Linda Partridge for sharing chemicals and instruments. The authors also acknowledge the sharing of HeLa, HEK293 cells from Nils-Göran Larsson's group. pCI-neo-FLAG is gift from Niels Gehring (University of Cologne). N2a-swe.10 cell line was kindly provided by Gopal Thinakaran (University of Chicago). The mouse sample used in this study was from the Transgenic Core Facility of the host institute. The authors thank Xiangru Xu for comments on the project at the early stage. The authors also appreciate Adam Antebi and Gabriella B Lundkvist for reading the manuscript.

Conflict of interest.

None declared.

References:

Abe N, Matsumoto K, Nishihara M, Nakano Y, Shibata A, Maruyama H, Shuto S, Matsuda A, Yoshida M, Ito Y et al. 2015. Rolling Circle Translation of Circular RNA in Living Human Cells. *Sci Rep* **5**: 16435.

Ashwal-Fluss R, Meyer M, Pamudurti NR, Ivanov A, Bartok O, Hanan M, Evantal N, Memczak S, Rajewsky N, Kadener S. 2014. circRNA biogenesis competes with pre-mRNA splicing. *Mol Cell* **56**: 55-66.

Brinster RL, Allen JM, Behringer RR, Gelinas RE, Palmiter RD. 1988. Introns increase transcriptional efficiency in transgenic mice. *Proc Natl Acad Sci U S A* **85**: 836-840.

Buchman AR, Berg P. 1988. Comparison of intron-dependent and intron-independent gene expression. *Mol Cell Biol* **8**: 4395-4405.

Chen CY, Sarnow P. 1995. Initiation of protein synthesis by the eukaryotic translational apparatus on circular RNAs. *Science* **268**: 415-417.

Chen LL. 2016. The biogenesis and emerging roles of circular RNAs. *Nat Rev Mol Cell Biol* **17**: 205-211.

Choi T, Huang M, Gorman C, Jaenisch R. 1991. A generic intron increases gene expression in transgenic mice. *Mol Cell Biol* **11**: 3070-3074.

Cox J, Neuhauser N, Michalski A, Scheltema RA, Olsen JV, Mann M. 2011. Andromeda: a peptide search engine integrated into the MaxQuant environment. *J Proteome Res* **10**: 1794-1805.

Gallegos JE, Rose AB. 2015. The enduring mystery of intron-mediated enhancement. *Plant Sci* **237**: 8-15.

Gruner H, Cortes-Lopez M, Cooper DA, Bauer M, Miura P. 2016. CircRNA accumulation in the aging mouse brain. *Sci Rep* **6**: 38907.

Guarnerio J, Bezzi M, Jeong JC, Paffenholz SV, Berry K, Naldini MM, Lo-Coco F, Tay Y, Beck AH, Pandolfi PP. 2016. Oncogenic Role of Fusion-circRNAs Derived from Cancer-Associated Chromosomal Translocations. *Cell* **165**: 289-302.

Hansen TB, Jensen TI, Clausen BH, Bramsen JB, Finsen B, Damgaard CK, Kjems J. 2013. Natural RNA circles function as efficient microRNA sponges. *Nature* **495**: 384-388.

Hentze MW, Preiss T. 2013. Circular RNAs: splicing's enigma variations. *EMBO J* **32**: 923-925.

Huang MT, Gorman CM. 1990. Intervening sequences increase efficiency of RNA 3' processing and accumulation of cytoplasmic RNA. *Nucleic Acids Res* **18**: 937-947.

Kristensen LS, Hansen TB, Veno MT, Kjems J. 2017. Circular RNAs in cancer: opportunities and challenges in the field. *Oncogene*.

Kulak NA, Pichler G, Paron I, Nagaraj N, Mann M. 2014. Minimal, encapsulated proteomic-sample processing applied to copy-number estimation in eukaryotic cells. *Nat Methods* **11**: 319-324.

Laxa M. 2016. Intron-Mediated Enhancement: A Tool for Heterologous Gene Expression in Plants? *Front Plant Sci* **7**: 1977.

Legnini I, Bozzoni I. 2017. Chapter 14 - Circular RNAs Expression, Function, and Regulation in Neural Systems A2 - Tonelli, Davide De Pietri. In *Essentials of Noncoding RNA in Neuroscience*, pp. 247-263. Academic Press.

Legnini I, Di Timoteo G, Rossi F, Morlando M, Briganti F, Sthandier O, Fatica A, Santini T, Andronache A, Wade M et al. 2017. Circ-ZNF609 Is a Circular RNA that Can Be Translated and Functions in Myogenesis. *Mol Cell* **66**: 22-37 e29.

Li X, Franz T. 2014. Up to date sample preparation of proteins for mass spectrometric analysis. *Arch Physiol Biochem* **120**: 188-191.

Liang D, Wilusz JE. 2014. Short intronic repeat sequences facilitate circular RNA production. *Genes Dev* **28**: 2233-2247.

Livak KJ, Schmittgen TD. 2001. Analysis of relative gene expression data using real-time quantitative PCR and the 2(-Delta Delta C(T)) Method. *Methods* **25**: 402-408.

Memczak S, Jens M, Elefsinioti A, Torti F, Krueger J, Rybak A, Maier L, Mackowiak SD, Gregersen LH, Munschauer M et al. 2013. Circular RNAs are a large class of animal RNAs with regulatory potency. *Nature* **495**: 333-338.

Palmiter RD, Sandgren EP, Avarbock MR, Allen DD, Brinster RL. 1991. Heterologous introns can enhance expression of transgenes in mice. *Proc Natl Acad Sci U S A* **88**: 478-482.

Pamudurti NR, Bartok O, Jens M, Ashwal-Fluss R, Stottmeister C, Ruhe L, Hanan M, Wyler E, Perez-Hernandez D, Ramberger E et al. 2017. Translation of CircRNAs. *Mol Cell* **66**: 9-21 e27.

Piwecka M, Glazar P, Hernandez-Miranda LR, Memczak S, Wolf SA, Rybak-Wolf A, Filipchyk A, Klironomos F, Cerda Jara CA, Fenske P et al. 2017. Loss of a mammalian circular RNA locus causes miRNA deregulation and affects brain function. *Science*.

Rose AB, Beliakoff JA. 2000. Intron-mediated enhancement of gene expression independent of unique intron sequences and splicing. *Plant Physiol* **122**: 535-542.

Rybak-Wolf A, Stottmeister C, Glazar P, Jens M, Pino N, Giusti S, Hanan M, Behm M, Bartok O, Ashwal-Fluss R et al. 2015. Circular RNAs in the Mammalian Brain Are Highly Abundant, Conserved, and Dynamically Expressed. *Mol Cell* **58**: 870-885.

Schwab ME. 2010. Functions of Nogo proteins and their receptors in the nervous system. *Nat Rev Neurosci* **11**: 799-811.

Schwab ME, Strittmatter SM. 2014. Nogo limits neural plasticity and recovery from injury. *Curr Opin Neurobiol* **27**: 53-60.

Seiler S, Di Santo S, Widmer HR. 2016. Non-canonical actions of Nogo-A and its receptors. *Biochem Pharmacol* **100**: 28-39.

Starke S, Jost I, Rossbach O, Schneider T, Schreiner S, Hung LH, Bindereif A. 2015. Exon circularization requires canonical splice signals. *Cell Rep* **10**: 103-111.

Tatomer DC, Wilusz JE. 2017. An Unchartered Journey for Ribosomes: Circumnavigating Circular RNAs to Produce Proteins. *Mol Cell* **66**: 1-2.

Thinakaran G, Teplow DB, Siman R, Greenberg B, Sisodia SS. 1996. Metabolism of the "Swedish" amyloid precursor protein variant in neuro2a (N2a) cells. Evidence that cleavage at the "beta-secretase" site occurs in the golgi apparatus. *J Biol Chem* **271**: 9390-9397.

Veno MT, Hansen TB, Veno ST, Clausen BH, Grebing M, Finsen B, Holm IE, Kjems J. 2015. Spatio-temporal regulation of circular RNA expression during porcine embryonic brain development. *Genome Biol* **16**: 245.

Vicens Q, Westhof E. 2014. Biogenesis of Circular RNAs. *Cell* **159**: 13-14.

Wang Y, Wang Z. 2015. Efficient backsplicing produces translatable circular mRNAs. *RNA* **21**: 172-179.

Westholm JO, Miura P, Olson S, Shenker S, Joseph B, Sanfilippo P, Celniker SE, Graveley BR, Lai EC. 2014. Genome-wide analysis of drosophila circular RNAs reveals their structural and sequence properties and age-dependent neural accumulation. *Cell Rep* **9**: 1966-1980.

Xia S, Feng J, Chen K, Ma Y, Gong J, Cai F, Jin Y, Gao Y, Xia L, Chang H et al. 2017. CSCD: a database for cancer-specific circular RNAs. *Nucleic Acids Res*.

Yang Y, Fan X, Mao M, Song X, Wu P, Zhang Y, Jin Y, Yang Y, Chen LL, Wang Y et al. 2017. Extensive translation of circular RNAs driven by N6-methyladenosine. *Cell Res* **27**: 626-641.

You X, Vlatkovic I, Babic A, Will T, Epstein I, Tushev G, Akbalik G, Wang M, Glock C, Quedenau C et al. 2015. Neural circular RNAs are derived from synaptic genes and regulated by development and plasticity. *Nat Neurosci* **18**: 603-610.

Zhang XO, Wang HB, Zhang Y, Lu X, Chen LL, Yang L. 2014. Complementary sequence-mediated exon circularization. *Cell* **159**: 134-147.

Zhang Y, Xue W, Li X, Zhang J, Chen S, Zhang JL, Yang L, Chen LL. 2016. The Biogenesis of Nascent Circular RNAs. *Cell Rep* **15**: 611-624.

Intron-mediated enhancement boosts circRNA expression: a robust method for circRNA function exploration

Dingding Mo[#,*], Xinping Li[#]
#, Max Planck Institute for Biology of Ageing, Joseph-Stelzmann-Strasse 9b, 50931 Cologne, Germany
*, Corresponding author, Dingding Mo, Dingding.Mo@age.mpg.de

Supplementary method

Label-free quantitative proteomics

HEK293 cells individually transfected with pCircRNA-BE-Rtn4, pCircRNA-DMo-Rtn4 and the control empty plasmid were lysed and in-solution digested with trypsin according to the previously established method (Li and Franz 2014). Briefly, Cell pellets were heated and sonicated in lysis buffer (100 mM Tris-HCl, 6 M guanidine hydrochloride, 10 mM TCEP (Tris (2-carboxyethyl) phosphine), 40 mM CAA (chloroacetamide)). After centrifugation, the diluted supernatant was diluted and digested with trypsin (Promega, V5280) overnight and the resulted peptides were purified with C18-SD StrageTip (Kulak et al. 2014; Li and Franz 2014).

The peptides were analyzed using an Orbitrap QExactive HF mass spectrometer (Thermo Fisher Scientific) with a Nano-electrospray ion source, coupled with an EASY-nLC 1000 (Thermo Fisher Scientific) UHPLC. A 25-cm long reverse-phase C18 column with 75 µm inner diameter (PicoFrit, LC Packings) was used for separating peptides. The LC run lasted 150 min with a concentration of 6% solvent B (0.1% formic acid in 80% acetonitrile) increasing to 31% over 155 min and further to 50% over 20 min. The column was subsequently washed and re-equilibrated. MS spectra were acquired in a data-dependent manner with top 15. For MS, the mass range was set to 300−1800m/z and resolution to 60K at 200m/z. The AGC target of MS was set to 3e6, and the maximum injection time was 80 ms. Peptides were fragmented with HCD with collision energy of 27. The resolution was set to 15K. The AGC target of MSMS was 1e5 and the maximum injection time was 80 ms.

MaxQuant version 1.5.3.8 with integrated Andromeda search engine was used for analyzing the LC/MSMS raw data (Cox et al. 2011; Kulak et al. 2014). The raw data were searched against the mouse proteome from UniProt (knowledgebase 2016_04). Following parameters were used for data analysis: for ''fixed modification'': cysteine carbamidomethylation, methionine oxidation; for ''variable modification'': methionine oxidation and protein N-terminal acetylation; for ''digestion'' specific with Trypsin/P, Max. missed cleavages 2; for label-free quantification, match between runs is selected. Other parameters were set as default.

Protein quantification significant analysis was performed with the Perseus statistical framework (http://www.perseus-framework.org/) version 1.5.2.4. After removing the contaminants and reverse identifications, the intensities were transformed to log2. Two-sample test was performed to identify the differentially expressed proteins. Proteins with a p-value of less than 0.05 were designated as significantly differentially expressed.

References:

Cox J, Neuhauser N, Michalski A, Scheltema RA, Olsen JV, Mann M. 2011. Andromeda: a peptide search engine integrated into the MaxQuant environment. *J Proteome Res* **10**: 1794-1805.

Kulak NA, Pichler G, Paron I, Nagaraj N, Mann M. 2014. Minimal, encapsulated proteomic-sample processing applied to copy-number estimation in eukaryotic cells. *Nat Methods* **11**: 319-324.

Li X, Franz T. 2014. Up to date sample preparation of proteins for mass spectrometric analysis. *Arch Physiol Biochem* **120**: 188-191.

Supplementary table

Oligos used in this study

For mouse Rtn4 circRNA qRT-PCR	
Rtn4-c-F	AGTACTTACGAAAGAAGCAGAGG
Rtn4-c-R	GTATCACAGGCTCAGATGCAG
For mouse Rtn4 circRNA verification	
Rtn4-VF	CTCTTGTATAGCTTCTGATGTCTGGACC
Rtn4-VR	ACAGCTTTGCCCATCATTTGAG
For mouse Rtn4 mRNA qRT-PCR	
Rtn4-m-F2	GTTGGTGCCTTGTTCAATGG
Rtn4-m-R2	GCATCCTTAACGCTCTTGTTTG
For mouse β-Actin mRNA qRT-PCR	
ActbF1	ACCTTCTACAATGAGCTGCG
ActbR1	CTGGATGGCTACGTACATGG
For human β-Actin mRNA qRT-PCR	
Human ACTB-F	TCGTGCGTGACATTAAGGAG
Human ACTB-R	TTGCCAATGGTGATGACCTG
for pCircRNA-BE-Rtn4 vector construction	
i-Rtn4-BF	AATTAAGGATCCATGGGAATTCACGTGATTCTCC
i-Rtn4-XR	TTAATTCTCGAGCTACTAGAAAACACAGCTAACAGAATGC
lvRtn4I-BF	AATTAAGGATCCAACGTTAACCCTGTAATGAATACTG
lvRtn4I-XR	ACTTTGCTCGAGCTCATCAACATGACACAGTAGACATG
lvRtn4II-XF	ATGAGCTCGAGCAAAGTGATTTTCCACACAGTATTATCAC
lvRtn4II-XR	TTAATTCCCGGGCAACGTTAACCCTGTAATGAATACTG
For pCircRNA-Dmo-Rtn4 construction	
pCI-CMV-F	ATGTCCAATATGACCGCCATGTTG
pCI-Intron-R	aacgttgGATCCAGTCGACCTATAGTGAGTCGTATTAAGTACTCTAGCCTTAAGAGC

For multiple cloning sites insertion	
CicrI-F	CTATAGGTCGACTGGATCcaacgttaacc
CicrI-R	tctagaccgcggccgcgatatcgctagcagatctTCTCATctgaaaaacaaacagaataacaacctcag
CV-MCS-F	agatctgctagcgatatcgcggccgcggtctagaCTTCAGgtaataatccatgcaccgtctc
CV-MCS-R	cactttgCTCGAGctcatcaacatg
For overlap PCR in plasmid construction	
circDMO-LF	GTCGACTGGATCcaacgttaaccc
circDMO-LR	GCTGTCGTGGGAActgaaaaacaaacagaatacaacctcagc
circDMO-RF	TCAAGATGAAGTCGgtaataatccatgcaccgtctcacc
circDMO-RR	cactttgCTCGAGctcatcaacatg
For pCircRNA-DMo-Rtn4-FLAG construction	
circDMO-LF	GTCGACTGGATCcaacgttaaccc
Rtn4-FLAG-LR	cggtggcttgtcatcgtcgtccttgtagtcGGGTATCACAGGCTCAGATGCAGC
Rtn4-FLAG-RF	gactacaaggacgacgatgacaagccaccgTCCTCTGCAGgcaagttctttctgc
Rtn4-FLAG-RR	GCCCTCTCTGGCAATTCTCTAGAAGC
For pCircRNA-DMo-Rtn4-Stop construction	
circDMO-LF	GTCGACTGGATCcaacgttaaccc
Rtn4-Stop-LR	tcacggtggcttgtcatcgtcgtccttgtagtcGGGTATCACAGGCTCAGATGCAGC
Rtn4-FLAGS-RF	gactacaaggacgacgatgacaagccaccgtgaTCCTCTGCAGgcaagttctttctgc
Rtn4-FLAG-RR	GCCCTCTCTGGCAATTCTCTAGAAGC
For pCircRNA-IVS1-Rtn4 construction	
IVS1-LF-F	ATGTCCAATATGACCGCCATGTTG
IVS1-LF-R	gcaggcgactactctgtttctacaagaccagtttctatctgtctcattaagttgtgctgtaaaaaggataccaacCTGCCCAGTGCCTCACGACCAAC
IVS1-RF-F	ggtcttgtagaaacagagtagtcgcctgcttttctgccaggtgctgacttctctcccctgggctgttttcattttctcagGTGTCCACTCCCAGTTCAATTACAGCTC
IVS1-RF-R	gtttgtgccctggccacattccc
For pCircRNA-PAT1-Rtn4 construction	
IVS1-LF-F	ATGTCCAATATGACCGCCATGTTG

PAT1-intron 1-LF-R	ccacaaacaatttcaaaggatgtgtttttactctaataagcagacacctaaacccaaaaat cgaggctttacCTGCCCAGTGCCTCACGACCAAC
PAT1-intron 1-RF-F	gagtaaaaacacatcctttgaaattgtttgtggtcatttgattgtgctcttgatccattgaatt gctgcagGTGTCCACTCCCAGTTCAATTACAGCTC
IVS1-RF-R	gtttgtgccctggccacattccc

Intron-mediated enhancement boosts circRNA expression: a robust method for circRNA function exploration

Dingding Mo[#, *], Xinping Li[#]
#, Max Planck Institute for Biology of Ageing, Joseph-Stelzmann-Strasse 9b, 50931 Cologne, Germany
*, Corresponding author, Dingding Mo, Dingding.Mo@age.mpg.de

Supplementary figures

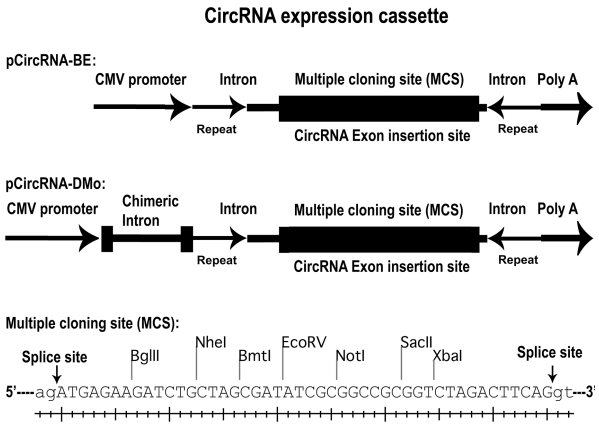

Supplementary Fig. 1 CircRNA expression cassette of pCircRNA-BE and pCircRNA-DMo vectors.
Multiple cloning site contain following restriction endonuclease sites: BglII, NheI, BmtI, EcoRV, NotI, SacII, XbaI. 5' and 3' splice site is indicated by arrow.

Intron-mediated enhancement boosts circRNA expression: a robust method for circRNA function exploration

Dingding Mo[#,] *, Xinping Li[#]
#, Max Planck Institute for Biology of Ageing, Joseph-Stelzmann-Strasse 9b, 50931 Cologne, Germany
*, Corresponding author, Dingding Mo, Dingding.Mo@age.mpg.de

Supplementary figures

Supplementary Fig. 2
17 mass spectrums of the tryptic peptides of Rtn4 circRNA derived protein
Left ordinate is the relative intensity, right ordinate is the absolute intensity,
Horizontal ordinate is m/z.

Supplementary Fig. 2

1 of 17 peptide mass spectrums

Scan	Method	Score	m/z
16346	FTMS; HCD	144.1	632.28

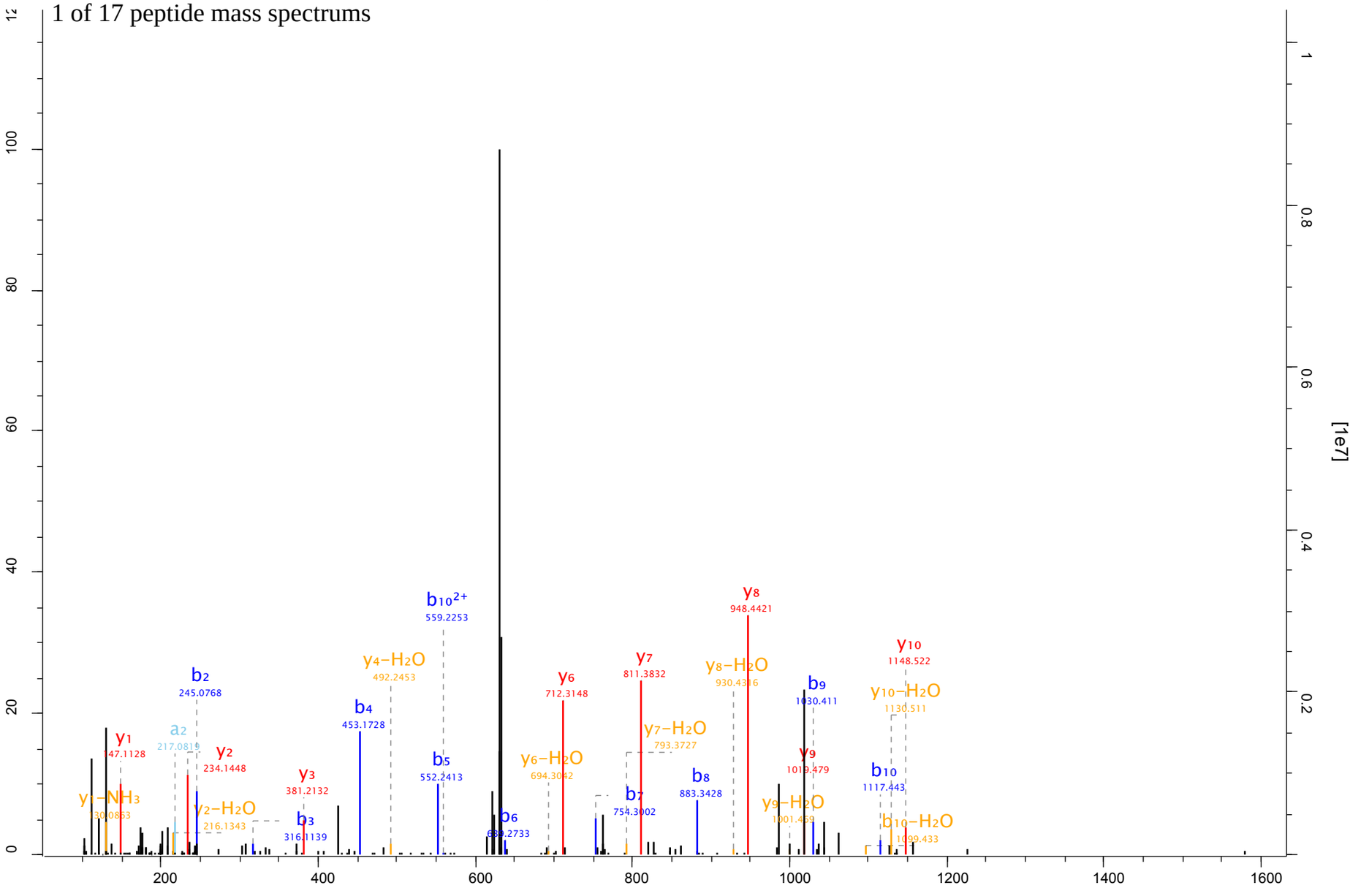

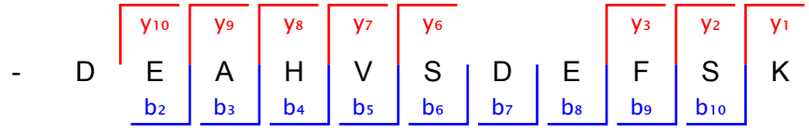

Supplementary Fig. 2

2 of 17 peptide mass spectrums

Scan	Method	Score	m/z
109034	FTMS; HCD	75.44	1089.21

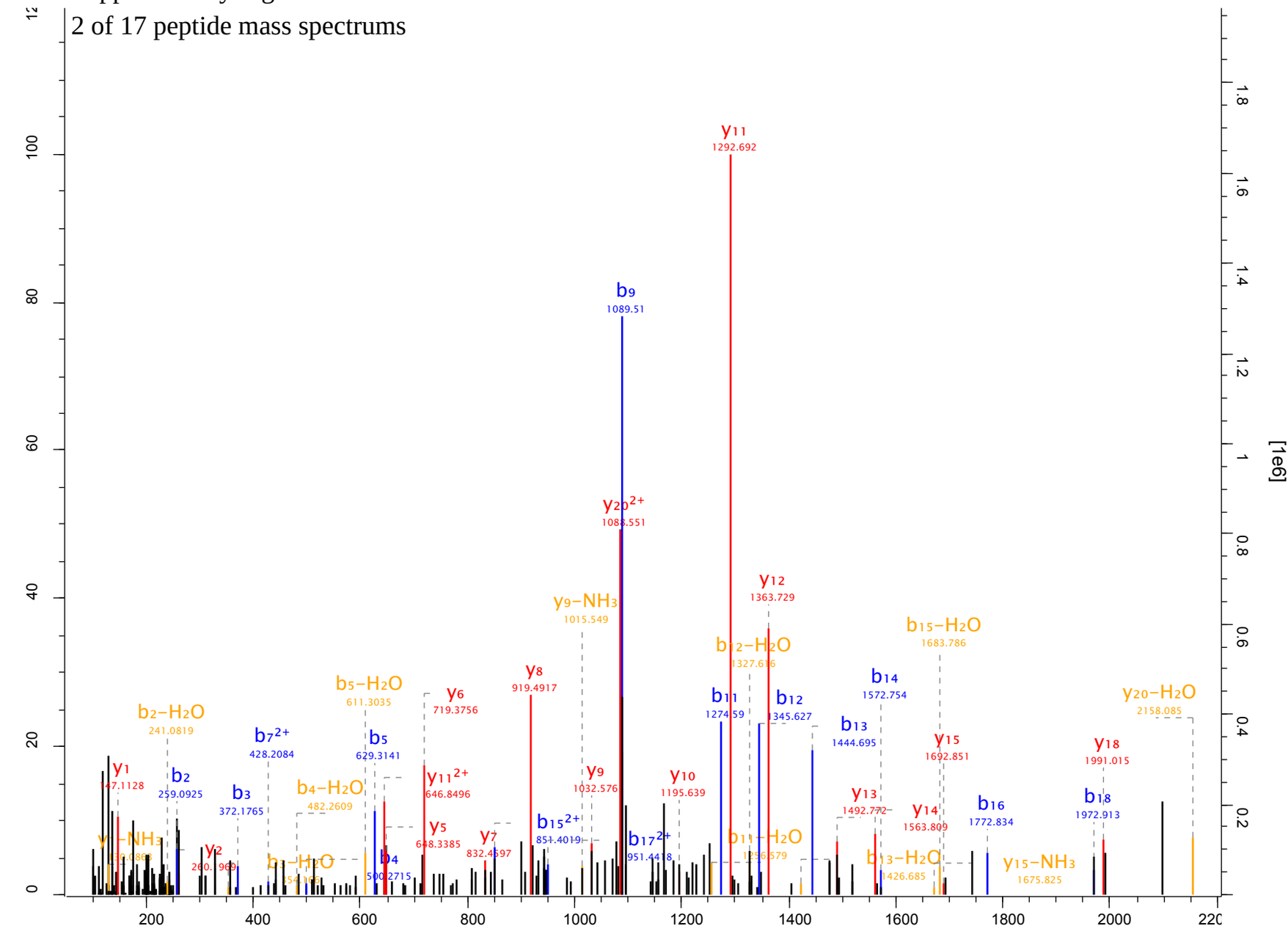

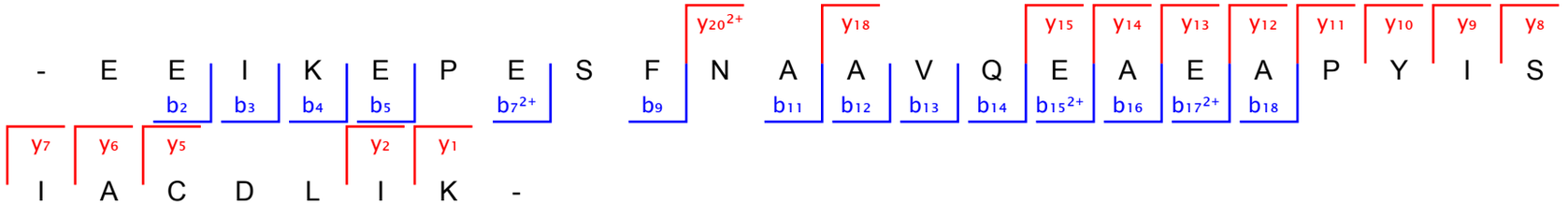

Supplementary Fig. 2
3 of 17 peptide mass spectrums

Scan	Method	Score	m/z
88482	FTMS; HCD	62.81	672.99

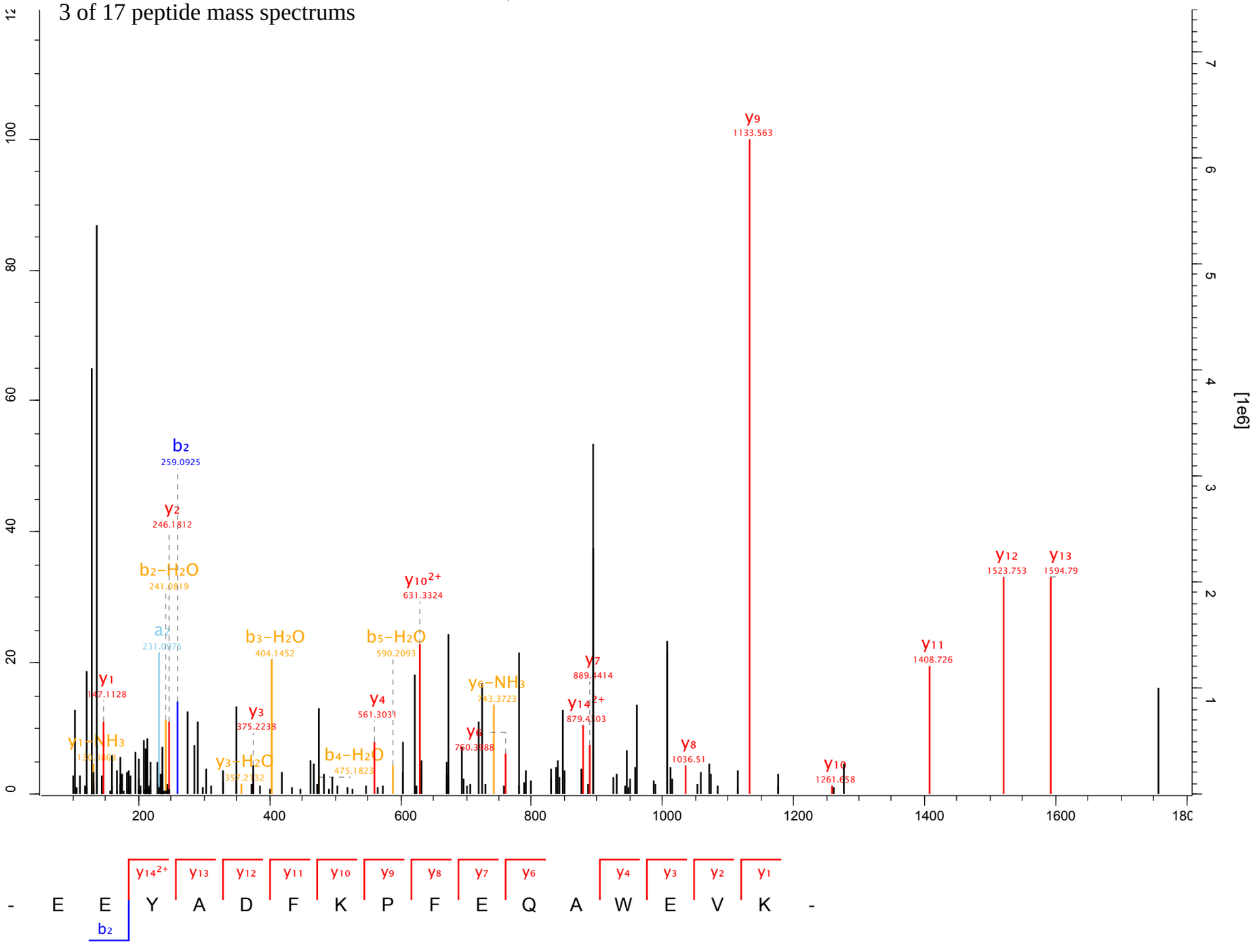

Supplementary Fig. 2
4 of 17 peptide mass spectrums

Scan	Method	Score	m/z
102956	FTMS; HCD	53.9	950.46

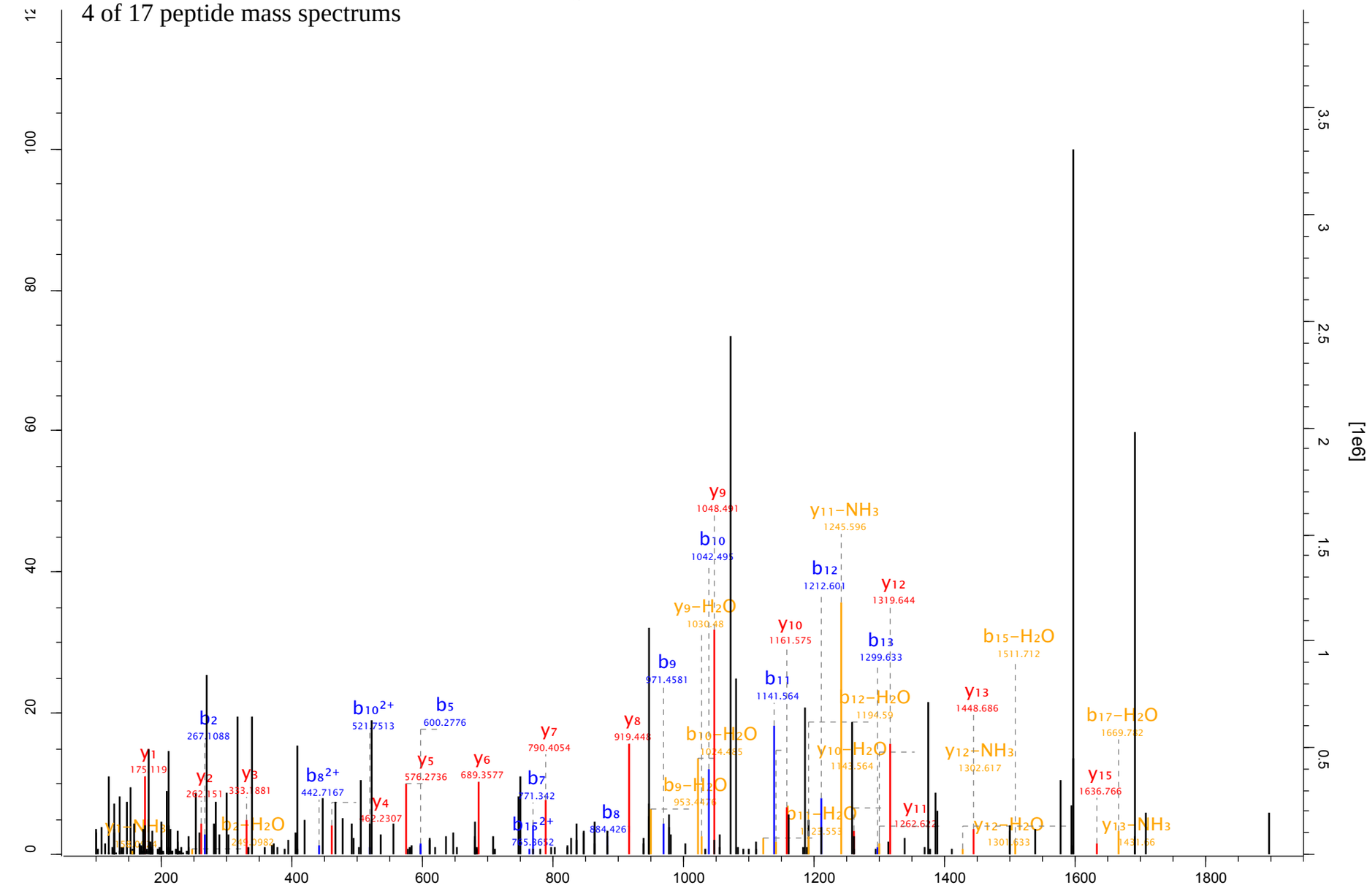

																	y15	y13	y12	y11	y10	y9	y8	y7	y6	y5	y4	y3				
-	E	H	G	Y	L	G	N	L	S	A	V	A	S	T	E	G	T	I	E	E	T	L	N	E	A						
		b2			b5		b7	b8	b9	b10	b11	b12	b13		b15 2+																	
y2	y1																														
S	R	-																													

Supplementary Fig. 2
5 of 17 peptide mass spectrums

Scan	Method	Score	m/z
114435	FTMS; HCD	80.69	1286.31

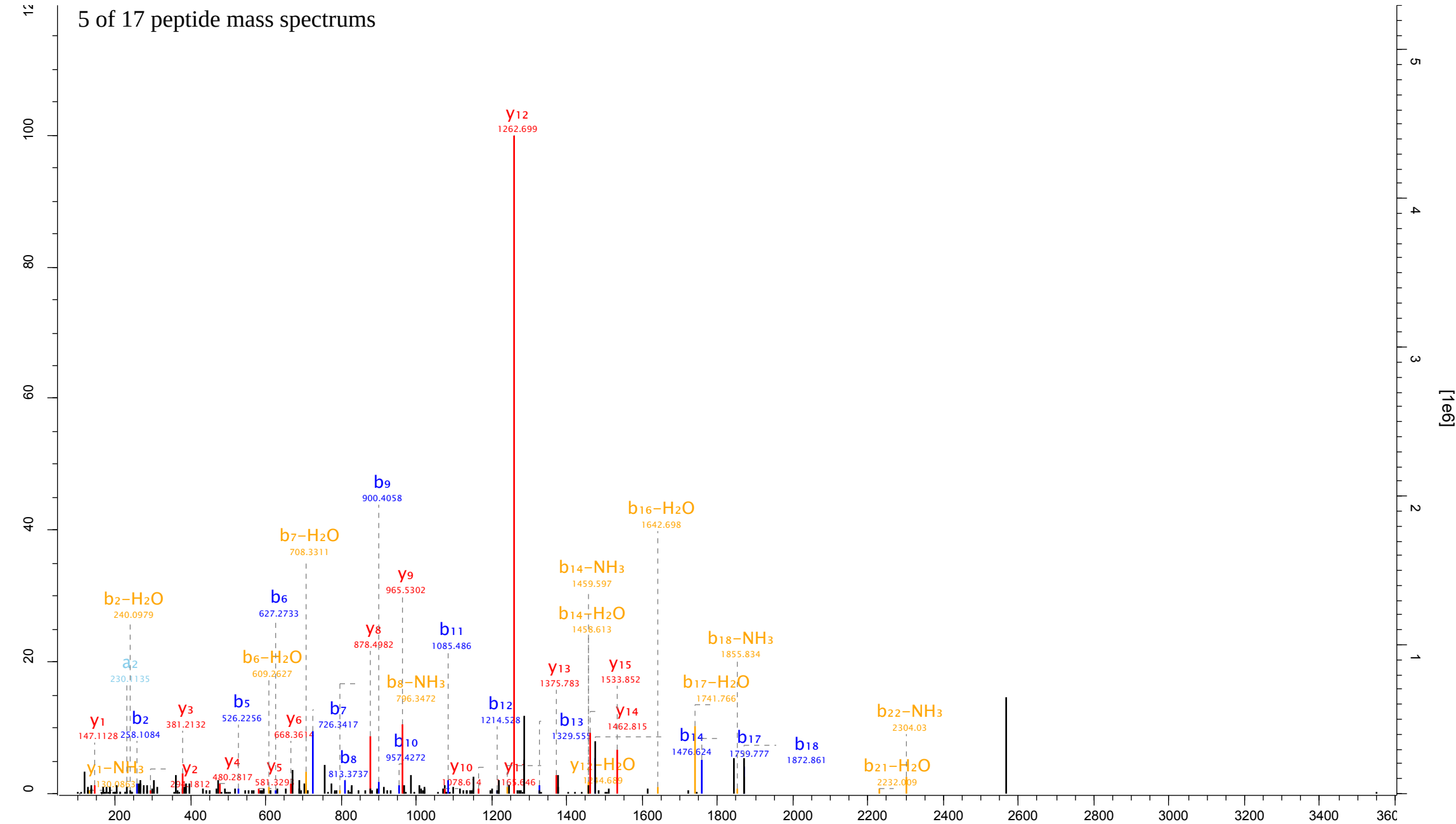

																									y15	y14	y13	y12	y11	y10					
-	E	Q	P	G	N	T	V	S	S	G	Q	E	D	F	P	S	V	L	F	E	T	A	A	S	L	P	S	L					
			b2			b5	b6	b7	b8	b9	b10	b11	b12	b13	b14			b17	b18															
y9	y8		y6	y5	y4	y3	y2	y1																										
S	P	L	S	T	V	S	F	K	-																									

Supplementary Fig. 2
6 of 17 peptide mass spectrums

Scan	Method	Score	m/z
40472	FTMS; HCD	69.26	529.93

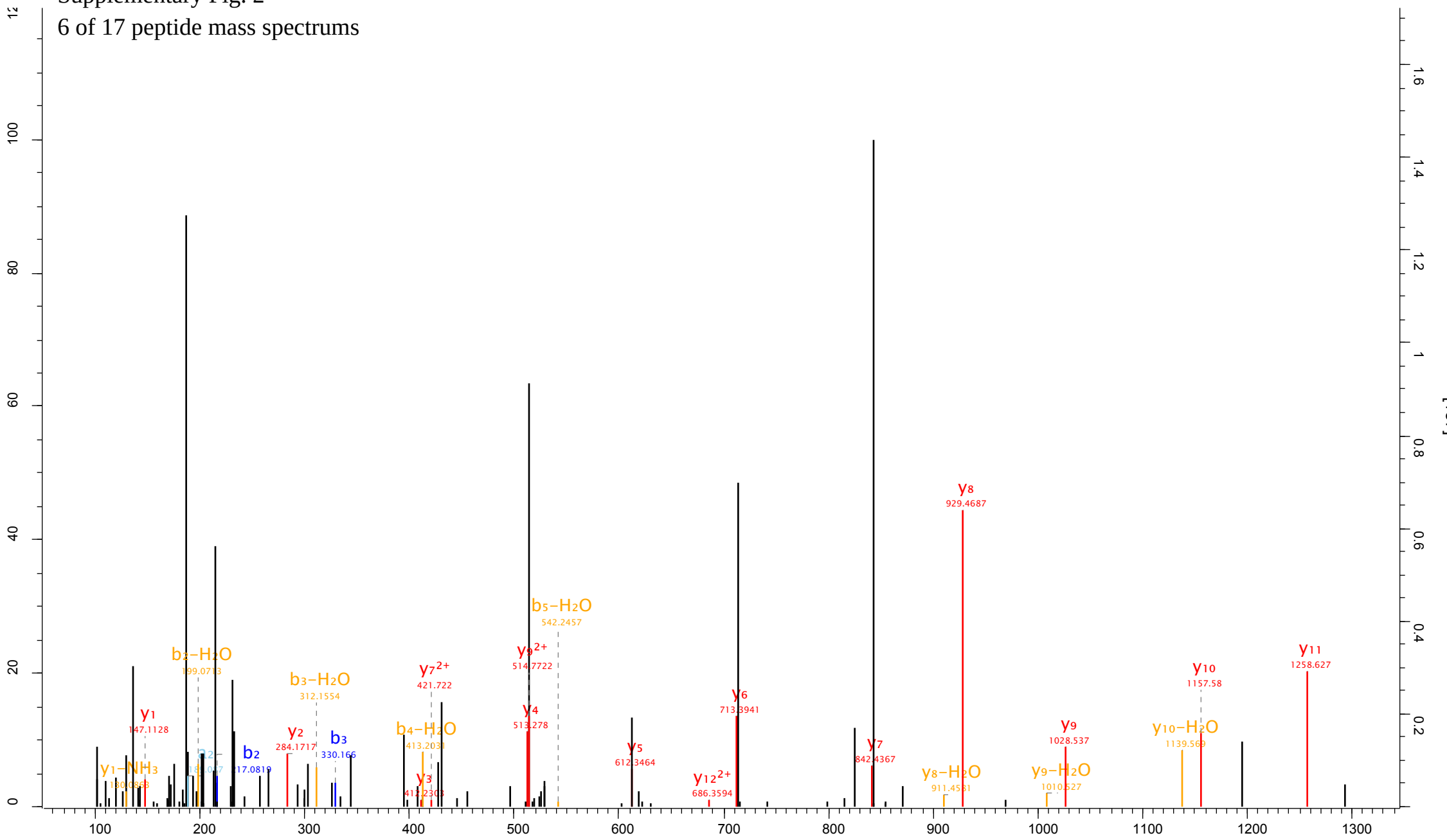

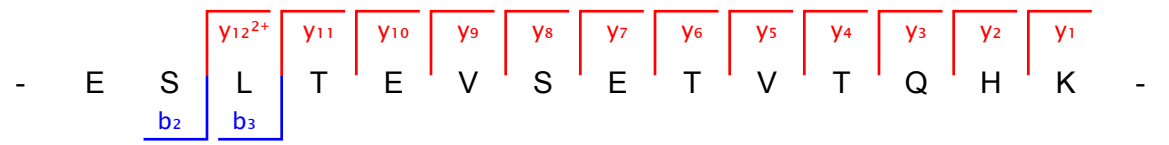

Supplementary Fig. 2

7 of 17 peptide mass spectrums

Scan	Method	Score	m/z
26668	FTMS; HCD	88.06	599.29

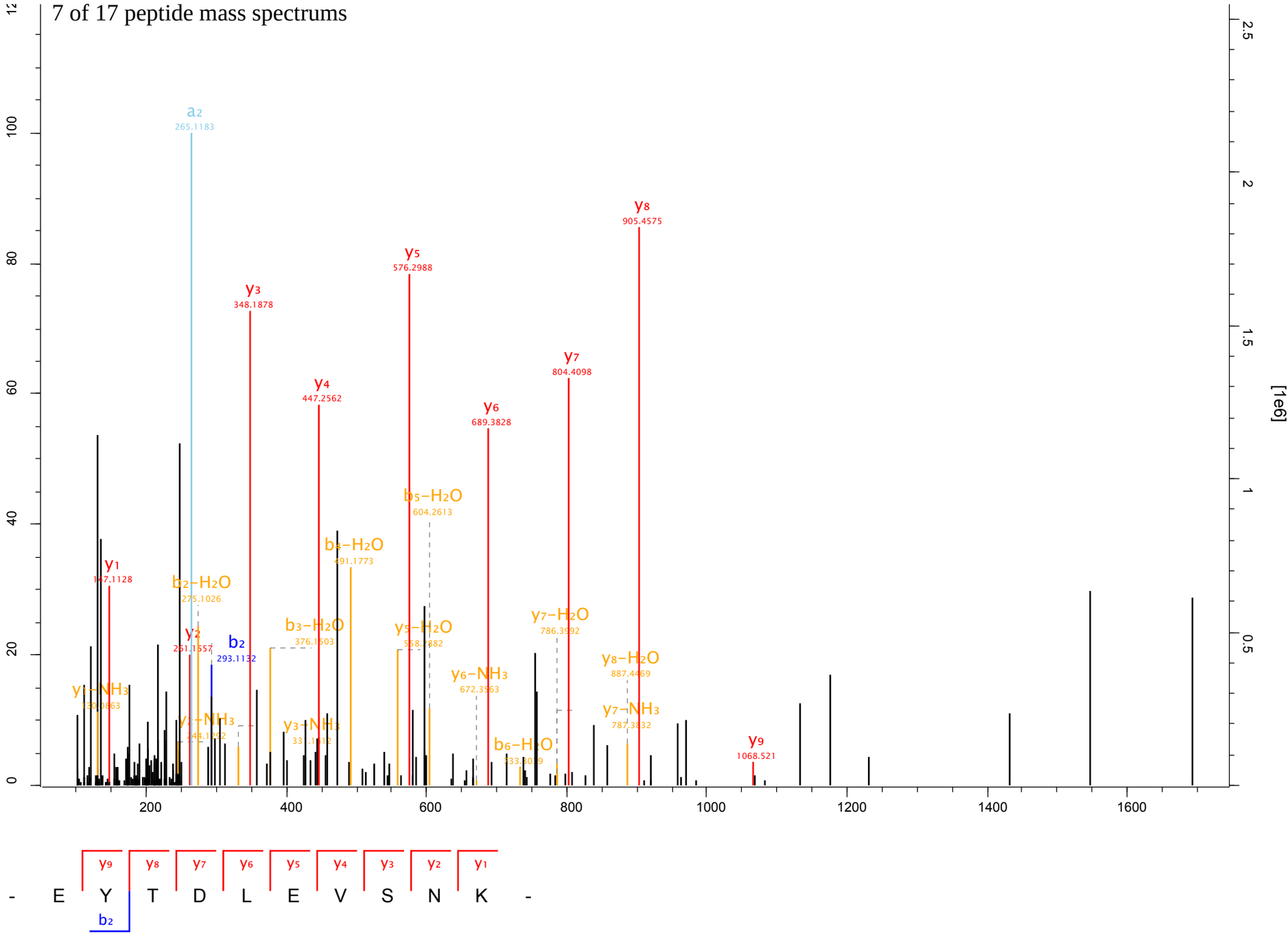

Supplementary Fig. 2

8 of 17 peptide mass spectrums

Scan	Method	Score	m/z	Gene names
21684	FTMS; HCD	73.41	589.65	NUDC

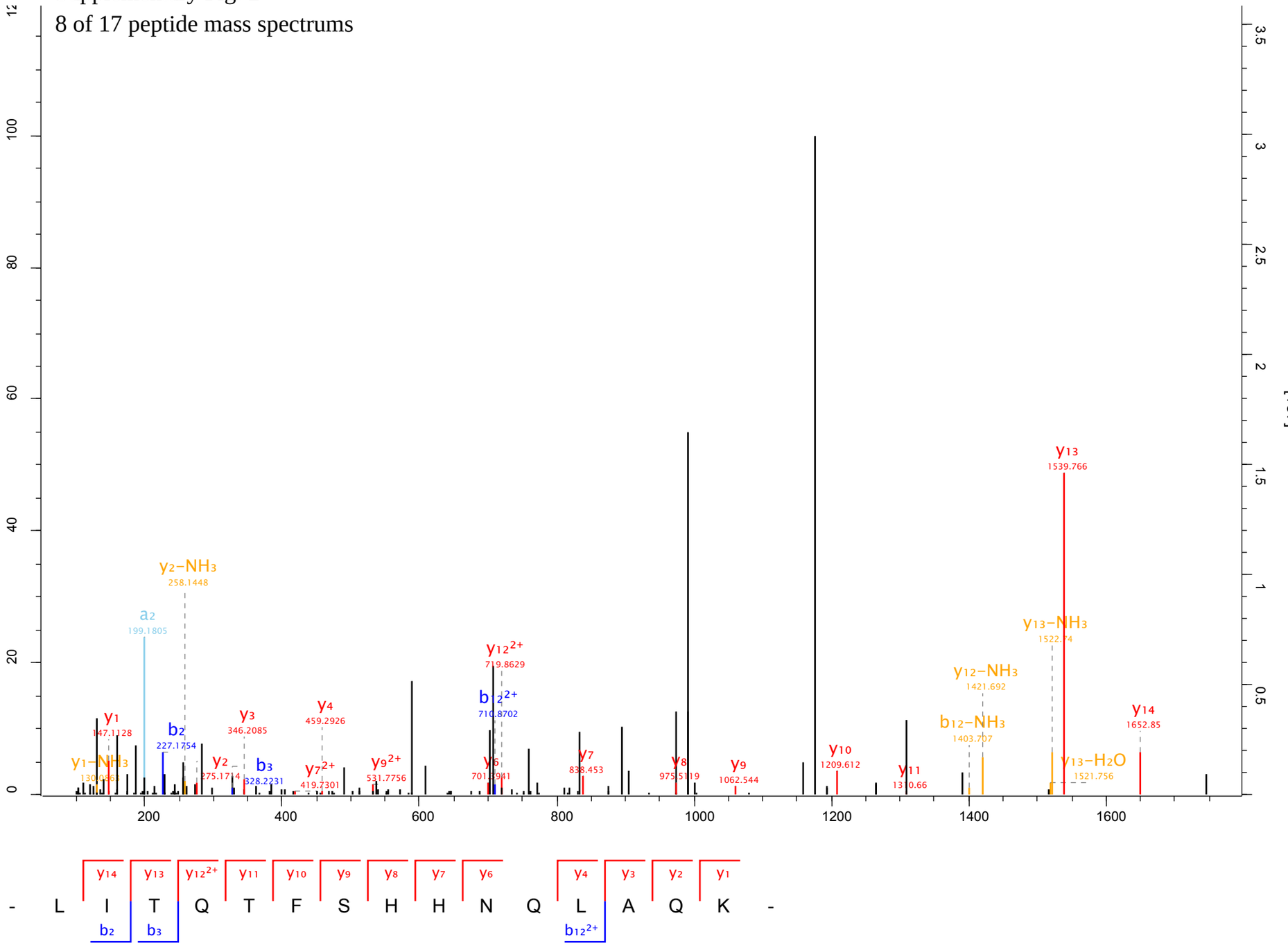

Supplementary Fig. 2

9 of 17 peptide mass spectrums

Scan	Method	Score	m/z
89618	FTMS; HCD	70.56	672.34

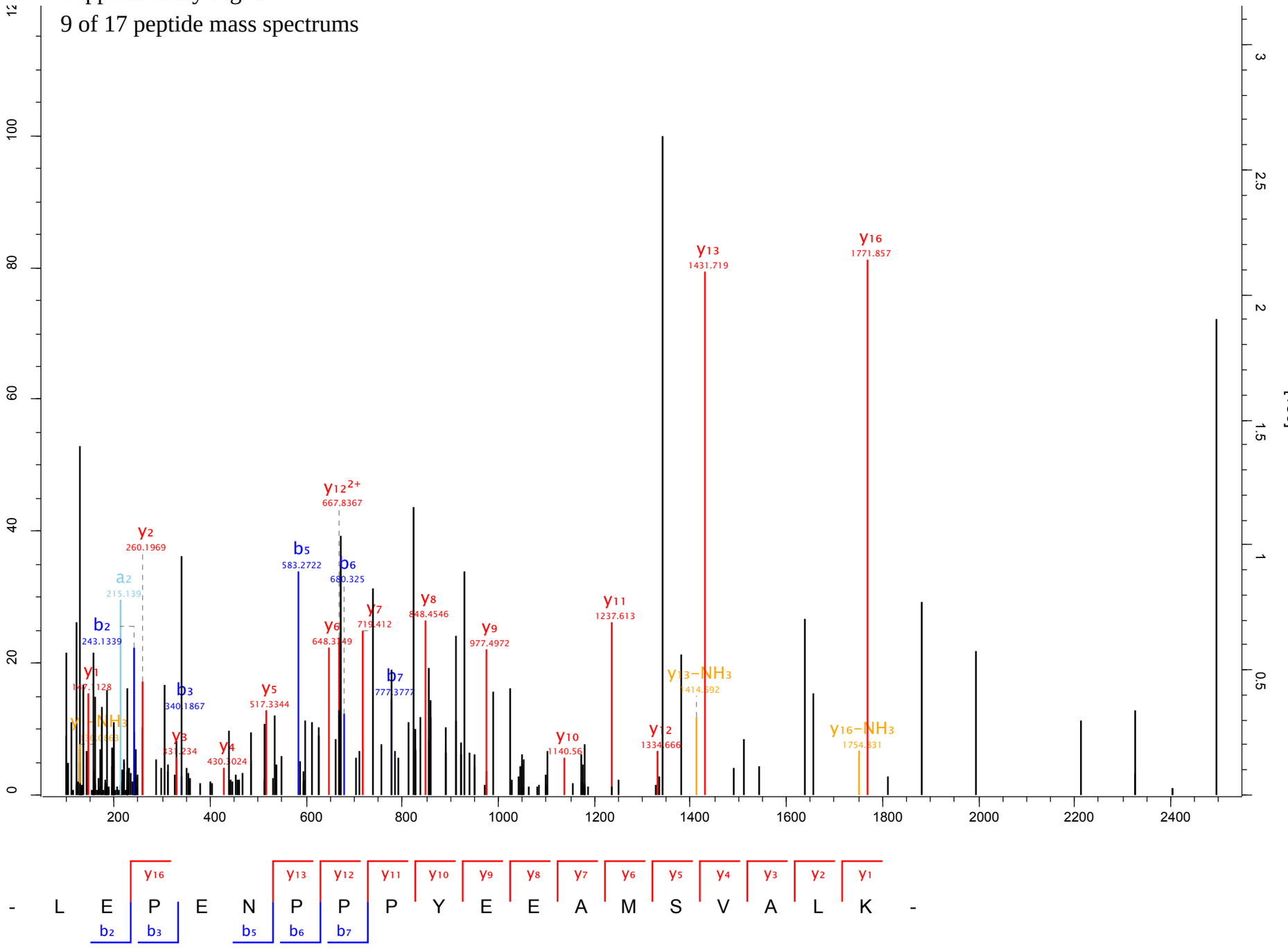

Supplementary Fig. 2

10 of 17 peptide mass spectrums

Scan	Method	Score	m/z
64737	FTMS; HCD	105.89	949.96

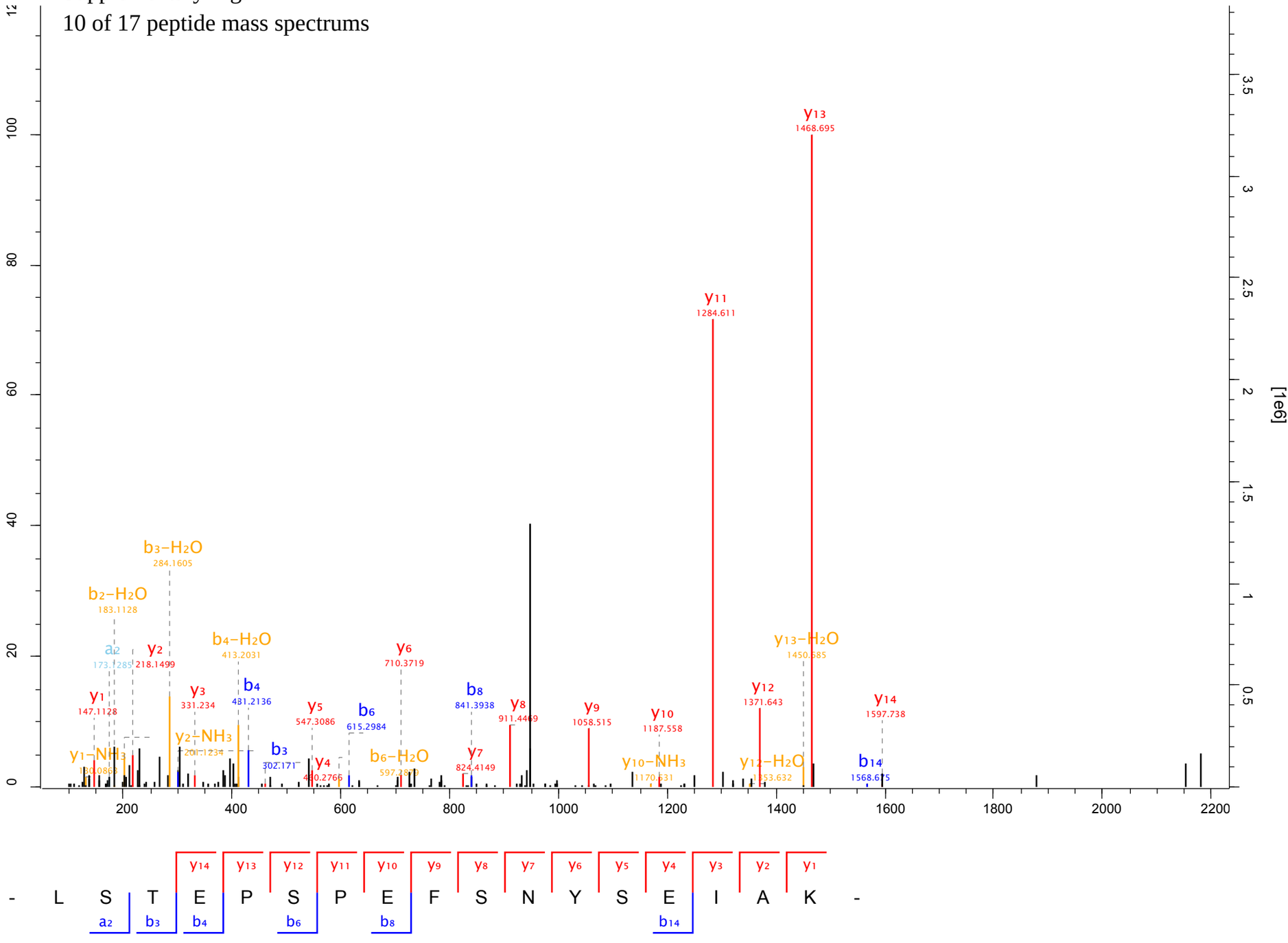

		y14	y13	y12	y11	y10	y9	y8	y7	y6	y5	y4	y3	y2	y1		
-	L	S	T	E	P	S	P	E	F	S	N	Y	S	E	I	A	K	-
		a2	b3	b4		b6		b8						b14			

Supplementary Fig. 2

11 of 17 peptide mass spectrums

Scan	Method	Score	m/z	Gene names
97064	FTMS; HCD	113.05	952.2	PTGES2

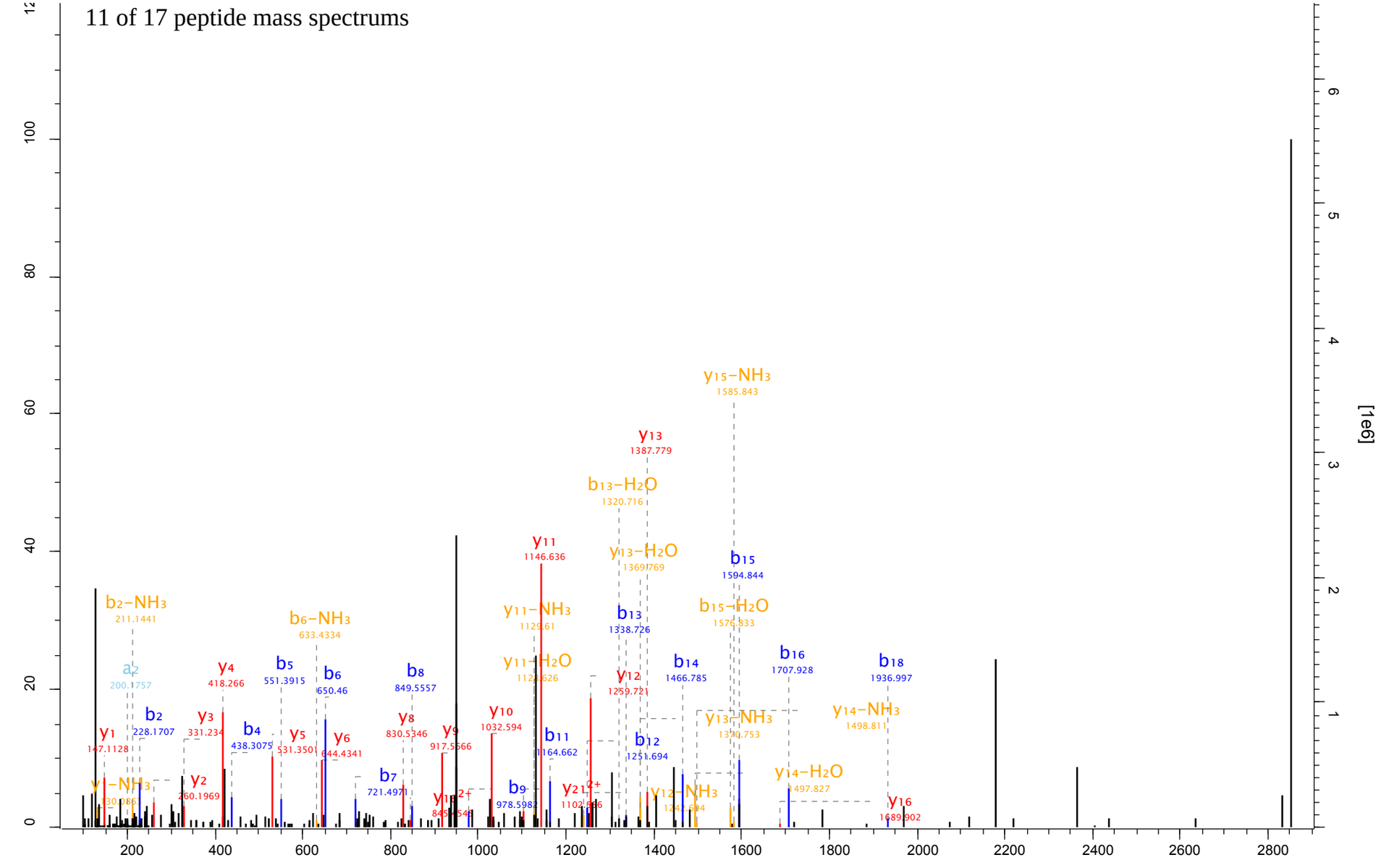

								y21 2+						y16			y13	y12	y11	y10	y9	y8		y6	y5	y4	y3						
-	K	V	P	I	L	V	A	Q	E	G	E	S	S	Q	Q	L	N	D	S	S	V	I	I	S	A							
		b2		b4	b5	b6	b7	b8	b9		b11	b12	b13	b14	b15	b16		b18														
y2	y1																															
L	K	-																														

Supplementary Fig. 2

12 of 17 peptide mass spectrums

Scan	Method	Score	m/z
58602	FTMS; HCD	146.59	766.89

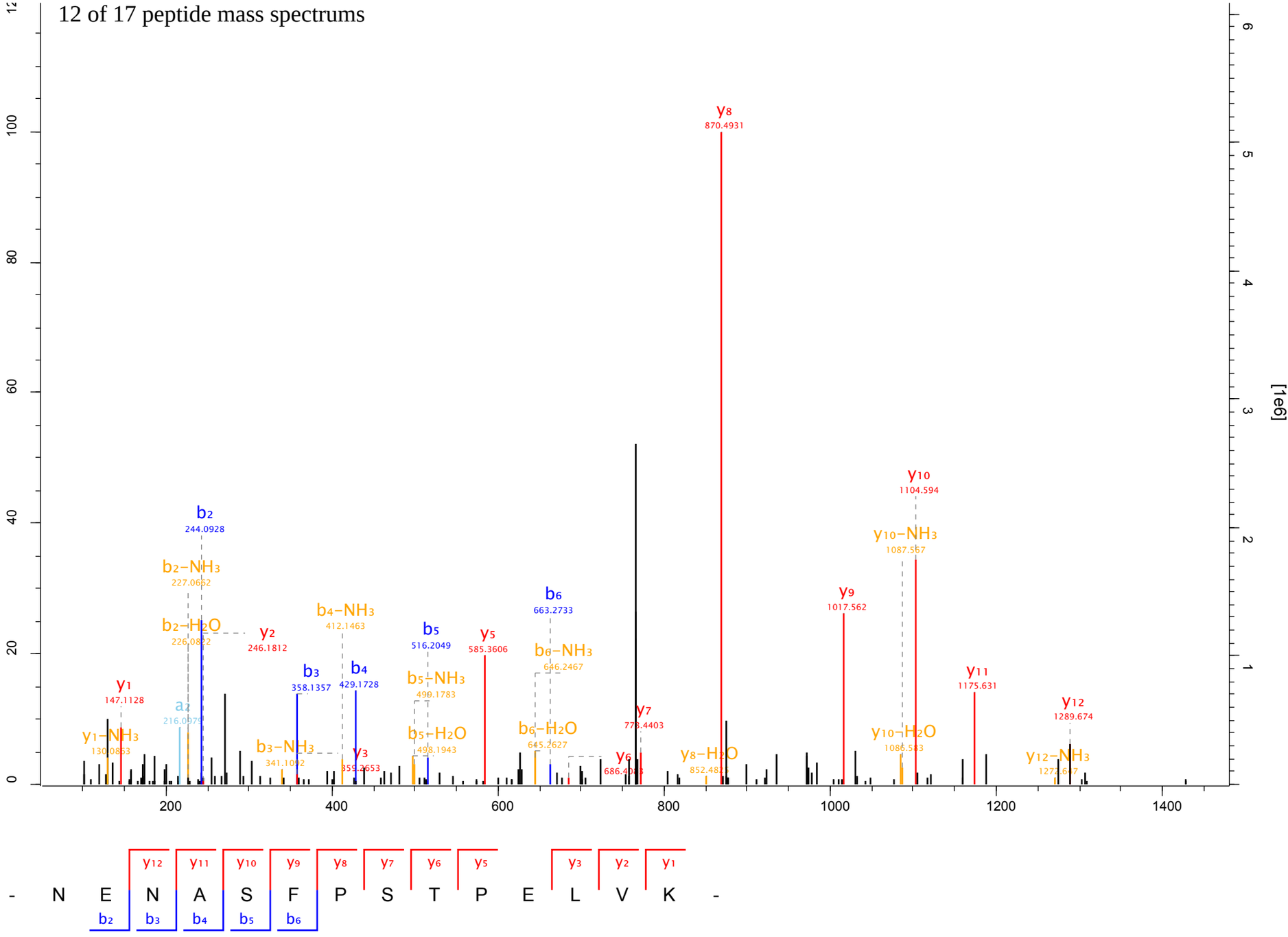

Supplementary Fig. 2

13 of 17 peptide mass spectrums

Scan	Method	Score	m/z
93362	FTMS; HCD	74.66	909.1

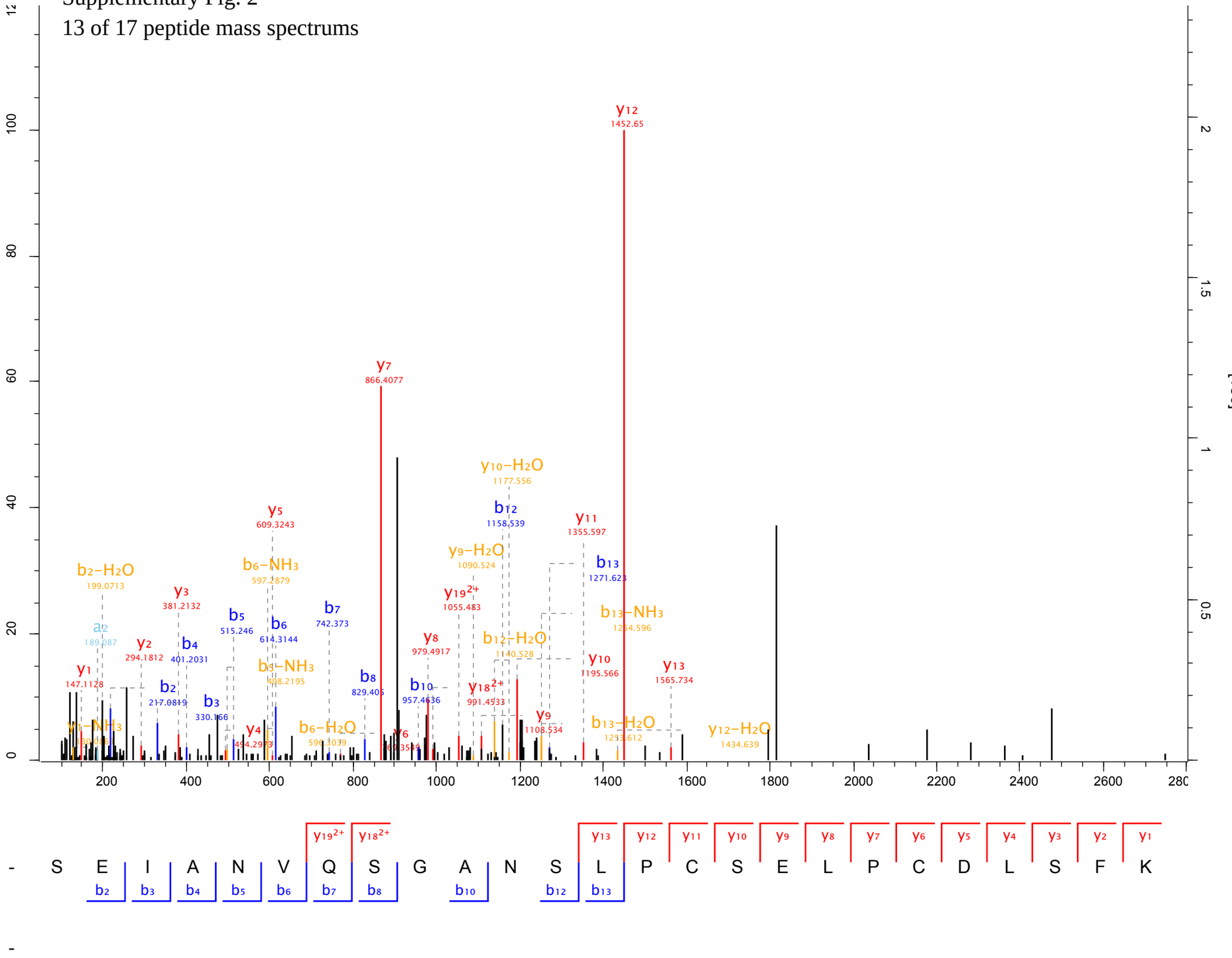

Supplementary Fig. 2
14 of 17 peptide mass spectrums

Scan	Method	Score	m/z
41459	FTMS; HCD	179.64	914.46

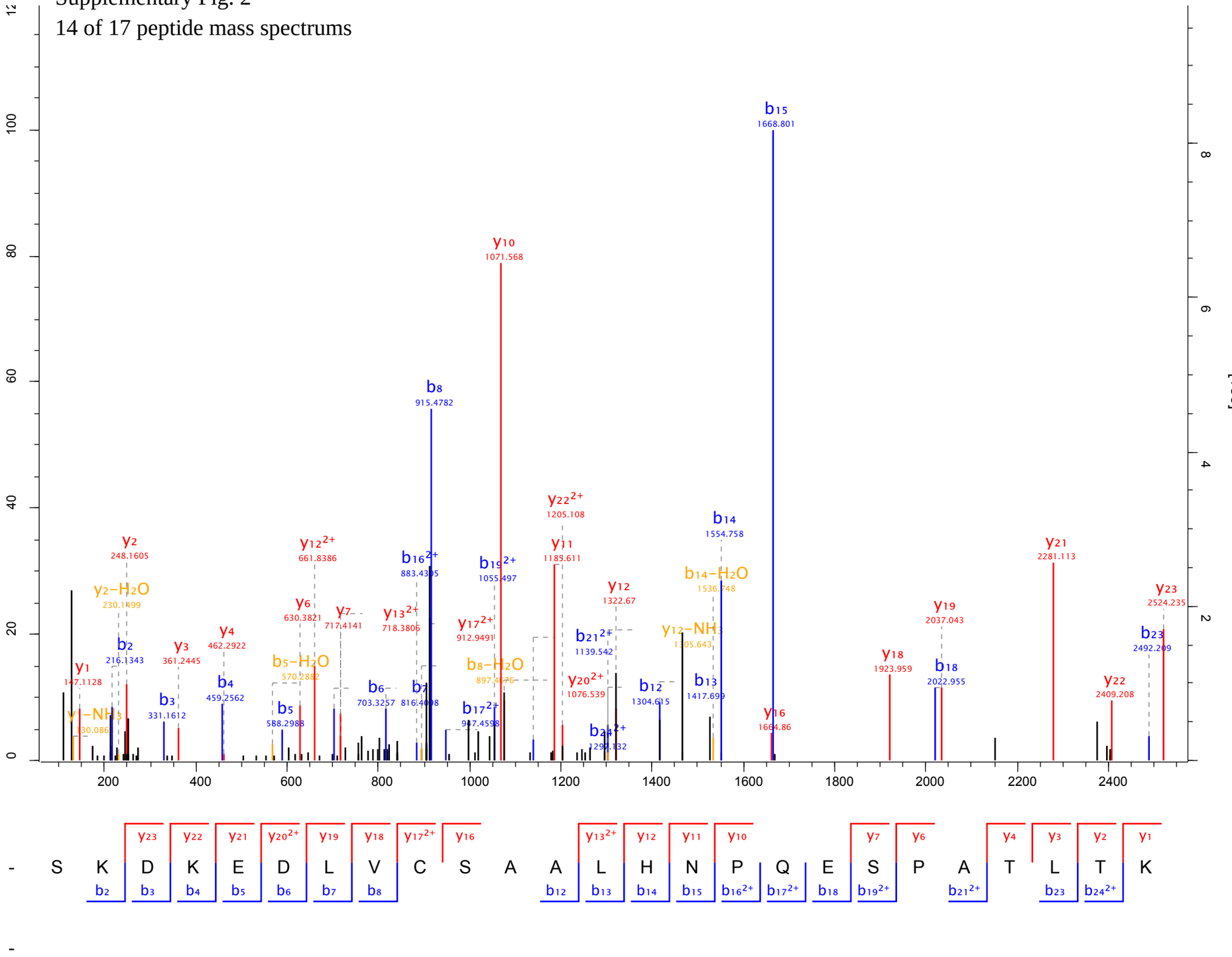

Supplementary Fig. 2

15 of 17 peptide mass spectrums

Scan	Method	Score	m/z
68376	FTMS; HCD	50.3	564.75

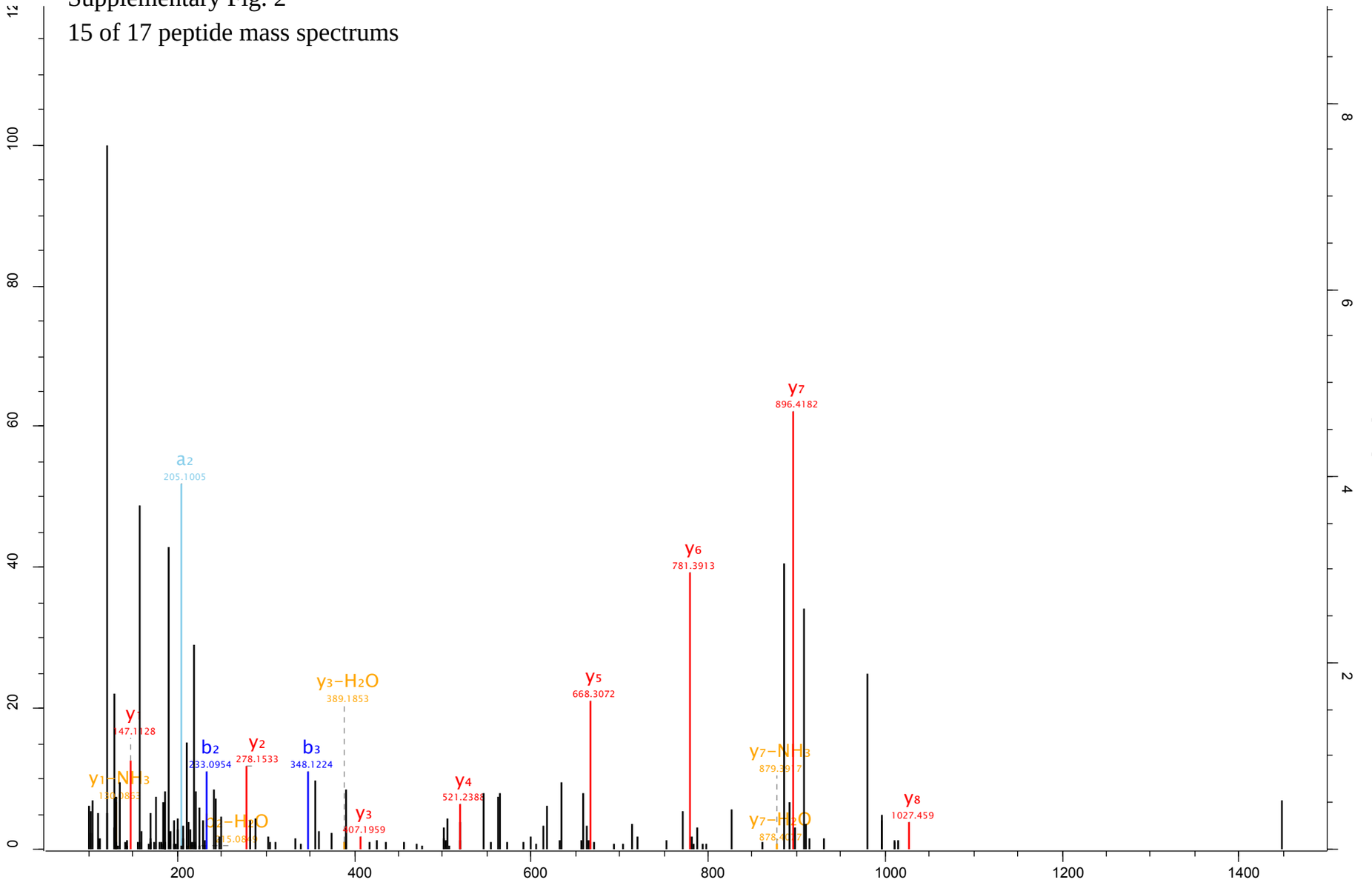

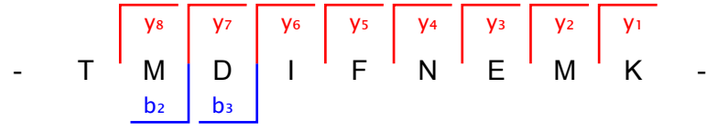

Supplementary Fig. 2

16 of 17 peptide mass spectrometry

Scan	Method	Score	m/z
109653	FTMS; HCD	163.18	864.16

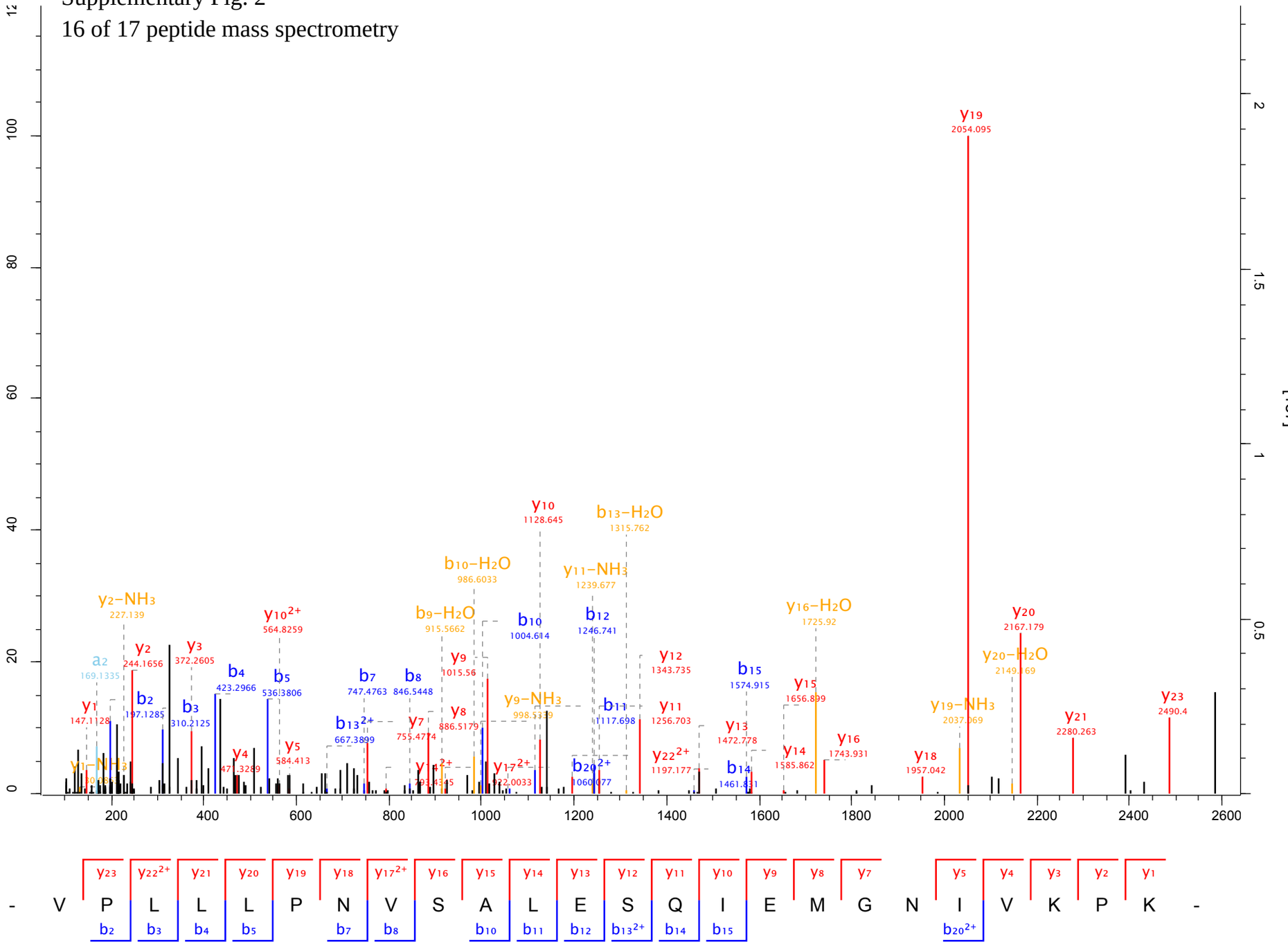

Supplementary Fig. 2

17 of 17 peptide mass spectrometry

Scan	Method	Score	m/z
11487	FTMS; HCD	114.21	659.34

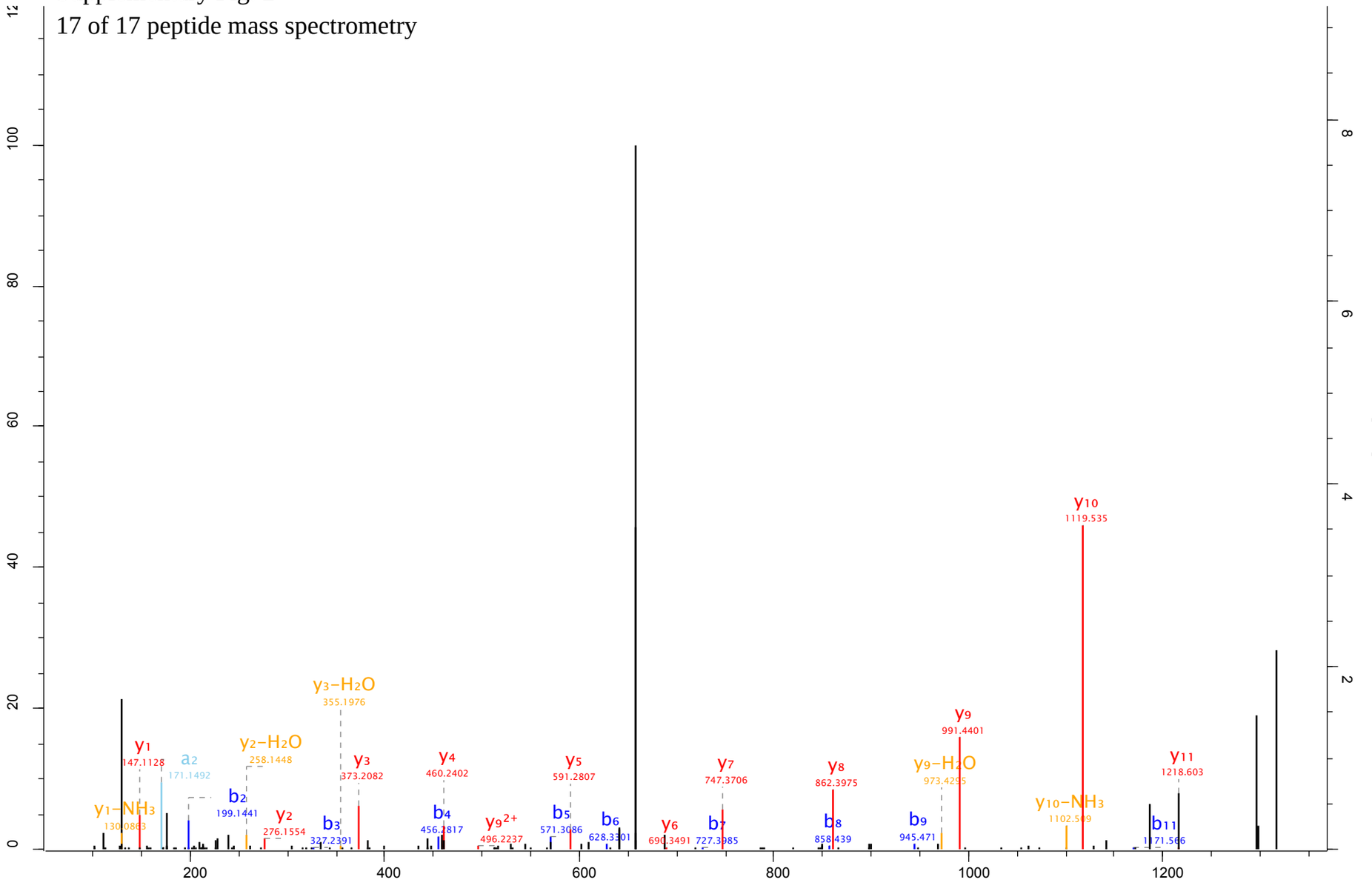

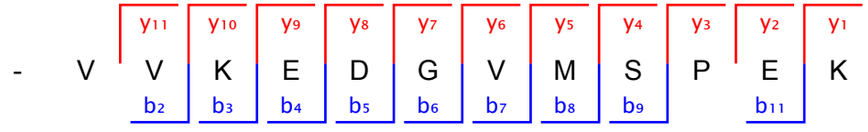

Supplementary Fig. 3

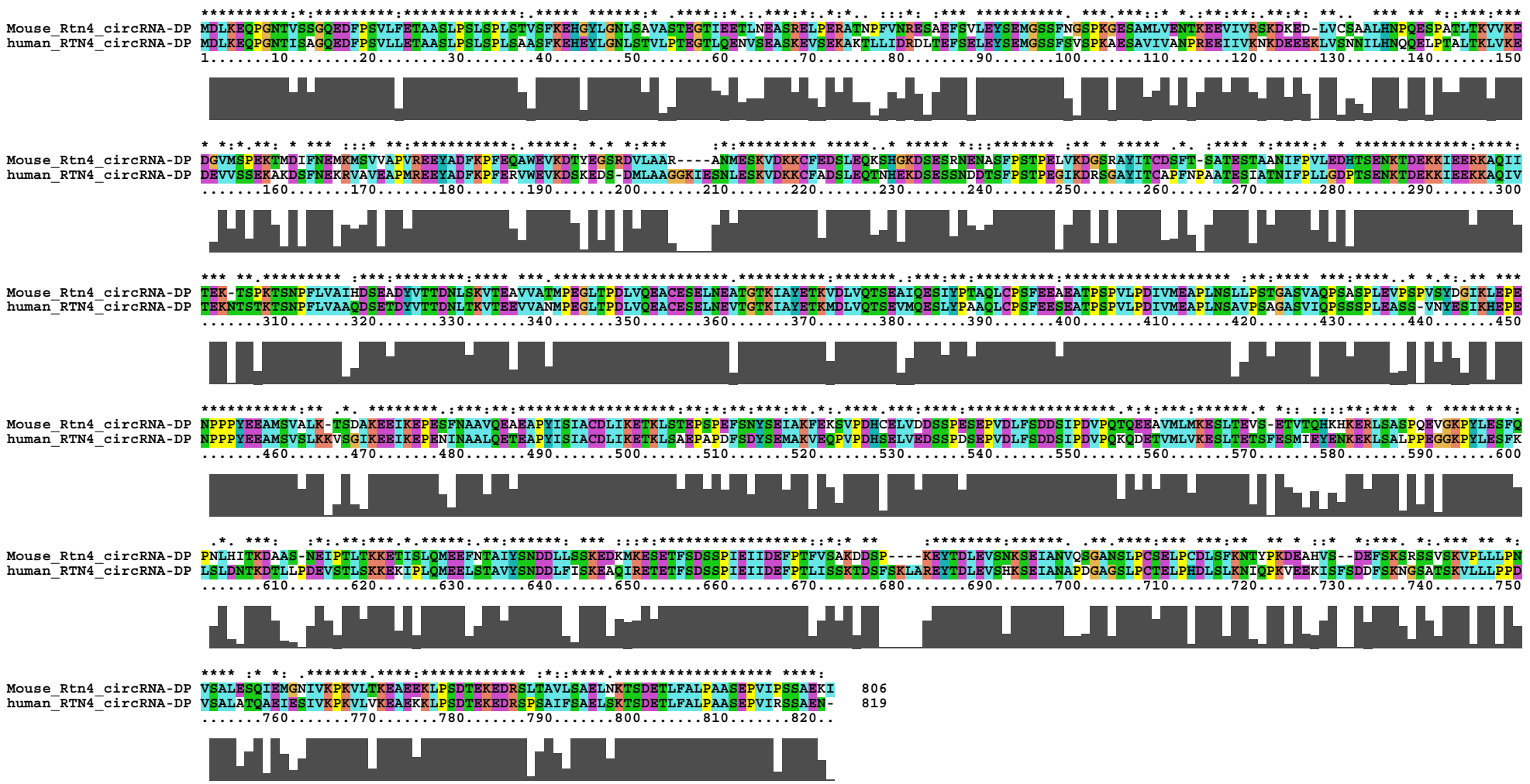

Supplementary Fig. 3. Alignment of RTN4 circRNA derived protein sequences from mouse and human.
The sequences of mouse Rtn4 circRNA derived protein (Mouse_Rtn4_circRNA-DP) and human Rtn4 circRNA derived protein (human_Rtn4_circRNA-DP) were aligned through ClustalX2.

Intron-mediated enhancement boosts circRNA expression: a robust method for circRNA function exploration

Dingding Mo[#, *], Xinping Li[#]
#, Max Planck Institute for Biology of Ageing, Joseph-Stelzmann-Strasse 9b, 50931 Cologne, Germany
*, Corresponding author, Dingding Mo, Dingding.Mo@age.mpg.de

Supplementary Figures

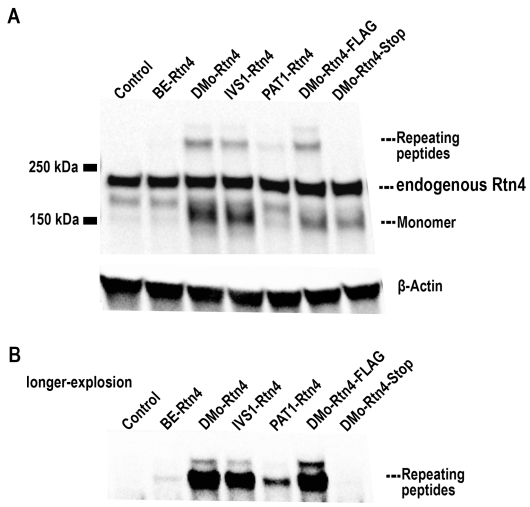

Supplementary Fig. 4 Rtn4 circRNA translation in N2a cells.
A. Western blot with Anti-Nogo A antibody of N2a cells with Rtn4 circRNA overexpression. Control, empty vector; BE-Rtn4, pCircRNA-BE-Rtn4; DMo-Rtn4, pCircRNA-DMo-Rtn4; IVS1-Rtn4, pCircRNA-IVS1-Rtn4; PAT1-Rtn4, pCircRNA-PAT1-Rtn4; DMo-Rtn4-FLAG, pCircRNA-DMo-Rtn4-FLAG; DMo-Rtn4-Stop, pCircRNA-DMo-Rtn4-Stop; the high molecular weight bands bigger than 250 kDa represent the repeating peptides from Rtn4 circRNA continuous translation; monomer is the single round Rtn4 circRNA translation product; actin is used as loading control. B. the longer explosion of the high molecular weight bands bigger than 250 kDa.